Naval Research Laboratory
Stennis Space Center, MS 39529-5004

NRL/MR/7174--98-8091

Normal-Incidence, High-Frequency Bottom Penetration in the Soft Gassy Sediment of Eckernförde Bay, Germany

MARCIA A. WILSON

Ocean Acoustics Branch
Acoustics Division

April 23, 1998

REPORT DOCUMENTATION PAGE

Form Approved
OBM No. 0704-0188

1. AGENCY USE ONLY *(Leave blank)*

2. REPORT DATE
April 23, 1998

3. REPORT TYPE AND DATES COVERED
Final

4. TITLE AND SUBTITLE
Normal-Incidence, High-Frequency Bottom Penetration in the Soft Gassy Sediment of Eckernförde Bay, Germany

5. FUNDING NUMBERS
Job Order No. 571506108
Program Element No. 0601153N
Project No.
Task No. 05391
Accession No. 153-059

6. AUTHOR(S)
Marcia A. Wilson

7. PERFORMING ORGANIZATION NAME(S) AND ADDRESS(ES)
Naval Research Laboratory
Acoustics Division
Stennis Space Center, MS 39529-5004

8. PERFORMING ORGANIZATION REPORT NUMBER
NRL/MR/7174--98-8091

9. SPONSORING/MONITORING AGENCY NAME(S) AND ADDRESS(ES)
Office of Naval Research
800 N. Quincy Street
Arlington, VA 22217-5000

10. SPONSORING/MONITORING AGENCY REPORT NUMBER

11. SUPPLEMENTARY NOTES

12a. DISTRIBUTION/AVAILABILITY STATEMENT
Approved for public release; distribution unlimited

12b. DISTRIBUTION CODE

13. ABSTRACT *(Maximum 200 words)*

Normal-incidence, high-frequency acoustic bottom penetration measurements were made in the gassy sediment of Eckernförde Bay, Germany. Measurements were made of water-sediment insertion loss and signal level as a function of frequency and hydrophone depth. Results showed that hydrophones located in a gassy sublayer had signal levels that were higher than the signal level at a hydrophone located just below the sediment-water interface. This increase in amplitude is attributed to reverberation from free methane bubbles excited near and above their resonant frequency.

14. SUBJECT TERMS
high frequency, acoustics, sediment, bubbles, Eckernförde Bay

15. NUMBER OF PAGES
50

16. PRICE CODE

17. SECURITY CLASSIFICATION OF REPORT	18. SECURITY CLASSIFICATION OF THIS PAGE	19. SECURITY CLASSIFICATION OF ABSTRACT	20. LIMITATION OF ABSTRACT
Unclassified	Unclassified	Unclassified	SAR

Normal-incidence, high-frequency bottom penetration in the soft gassy sediments of Eckernförde Bay, Germany

by Marcia A. Wilson
(Naval Research Laboratory, Code 7174, Bldg. 1005, Stennis Space Center, MS 39529)

Abstract: Normal-incidence high-frequency acoustic bottom penetration measurements were made in the gassy sediment of Eckernförde Bay, Germany. Measurements were made of water-sediment insertion loss and signal level as a function of frequency and hydrophone depth. Results showed that hydrophones located in a gassy sublayer had signal levels that were higher than the signal level at a hydrophone located just below the sediment-water interface. This increase in amplitude is attributed to reverberation from free methane bubbles excited near and above their resonant frequency.

Introduction

Normal-incidence, high-frequency bottom penetration data were collected in Eckernförde Bay, Germany, which has a soft, muddy bottom containing gas bubbles. [1] The experiment was accomplished along with several Coastal Benthic Boundary Layer (CBBL) experiments in June and July of 1994. The goals of the acoustic experiment were to obtain data on normal-incidence acoustic insertion loss across the water-sediment interface, estimates of transmission loss through the sediment as a function of depth and frequency, and a better understanding of the physics of acoustic penetration in soft gassy sediments. [2] Eckernförde Bay has been the site of numerous previous experiments, which provide bottom characterizations and environmental data in addition to that taken in connection with this experiment. [3,4]

Experiment

The experiment was conducted from the research vessel WFS PLANET in 20 to 30 m of water. A high-frequency acoustic source was deployed over the side and lowered below the hull. A stable three point mooring was used so that the vertical axis of the buried hydrophone array would closely coincide with the maximum response axis of the source. A hydrophone insertion tool was then used to push the hydrophones into the soft sediment directly beneath the source to the depths shown in Figure 1. [2]

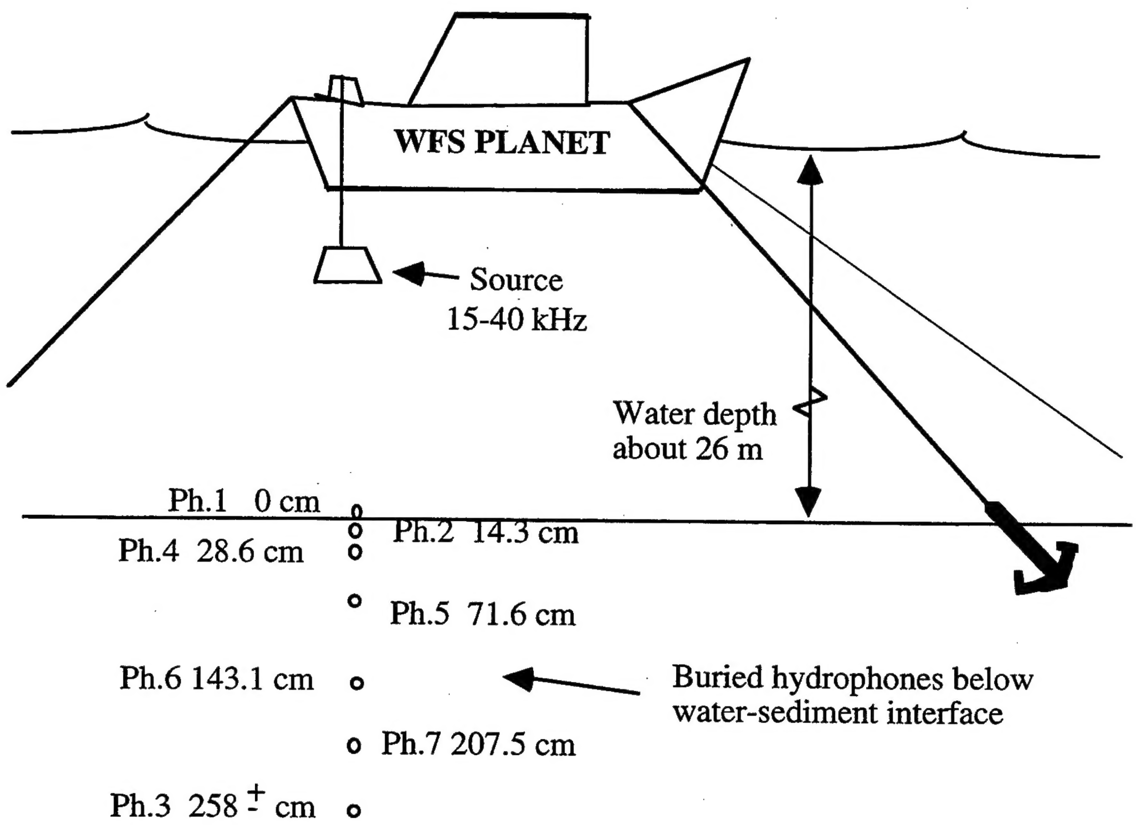

Figure 1. Configuration of sediment penetration experiment.

Signal pulses were transmitted at 15, 21, 25, 30, 35, and 40 kHz. At each frequency, continuous wave (CW) data for pulse lengths of 0.5, 1.0 and 5 ms were

collected. Each run consisted of data from all the hydrophones at a given frequency, pulse length and time period. Each run contained 128 pulses transmitted at 1 second intervals so that averages cover a little over two minutes. There were some initial problems in the early runs, so this report presents 0.5 and 1.0 ms pulse length data from runs 26 to 41.

Environmental measurements were made in support of the geoacoustic experiments. These included water temperature and salinity, core samples showing methane gas concentrations and depths, sediment properties, and side scan sonar profiles, [5,6,7,8]

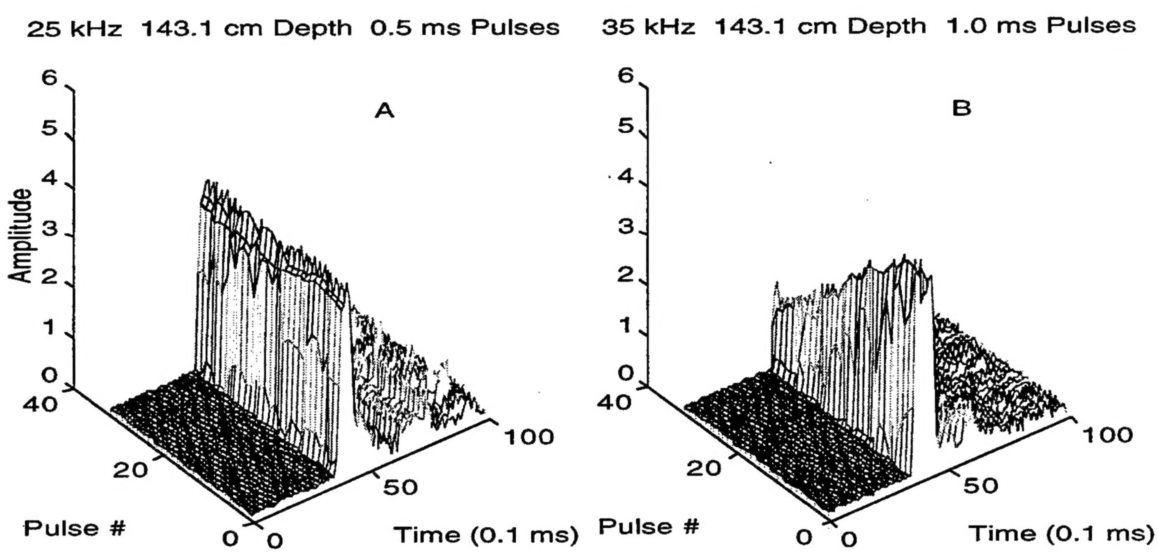

Figure 2. Waterfall plots of every 4th pulse in typical data sets.

Data Analysis

Data were base band heterodyned to a frequency of 5 kHz, sampled at 20 kHz, and stored on optical disks. Quadrature sampling facilitated calculation of a time series envelope for each received pulse. These envelopes have one sample every tenth of a millisecond. The data in envelope form were then formatted into files for

further processing. Sample plots of pulses for a given run were obtained. Using waterfall plots of every fourth pulse out of 128 collected, as shown in Figure 2, simplified data presentation. The average amplitude, in digitized units where 2048 units is equal to 5 volts, was determined and an average noise level present just before the pulse arrived was subtracted, then the result was converted to volts. Figure 3 shows typical uncalibrated mean pulse envelopes. (A complete set of gridded waterfall plots representing changes which occur from pulse to pulse in each run is presented in Appendix A and the uncalibrated mean pulse envelopes for each depth in each run analyzed are shown in Appendix B.)

In each mean pulse envelope, up to five or ten points, depending on the pulse length of the received direct arrival, were averaged to give an amplitude for each run. Originally each pulse was examined to be sure that only points within three dB of the peak direct arrival level were used, but after dozens of examples were compared, the results of the two methods were found to match within a couple tenths of a dB, so the average envelope for a run was used subsequently to determine which points were averaged. Conversion to decibels, calibrations, hydrophone sensitivities, and gains were applied to these mean levels before calculations of insertion losses were made and levels for different runs or depths within a run were compared.

To obtain the insertion loss, the mean level of the direct arrival peak at the hydrophone just below the surface (Ph.2) was subtracted from the mean level received at the hydrophone on the surface (Ph.1) (see Figure 1). Positive values indicate the amount of loss occurring at the water-sediment interface. Standard deviations of the data for each of these hydrophones were combined to give a standard deviation for each insertion loss value.

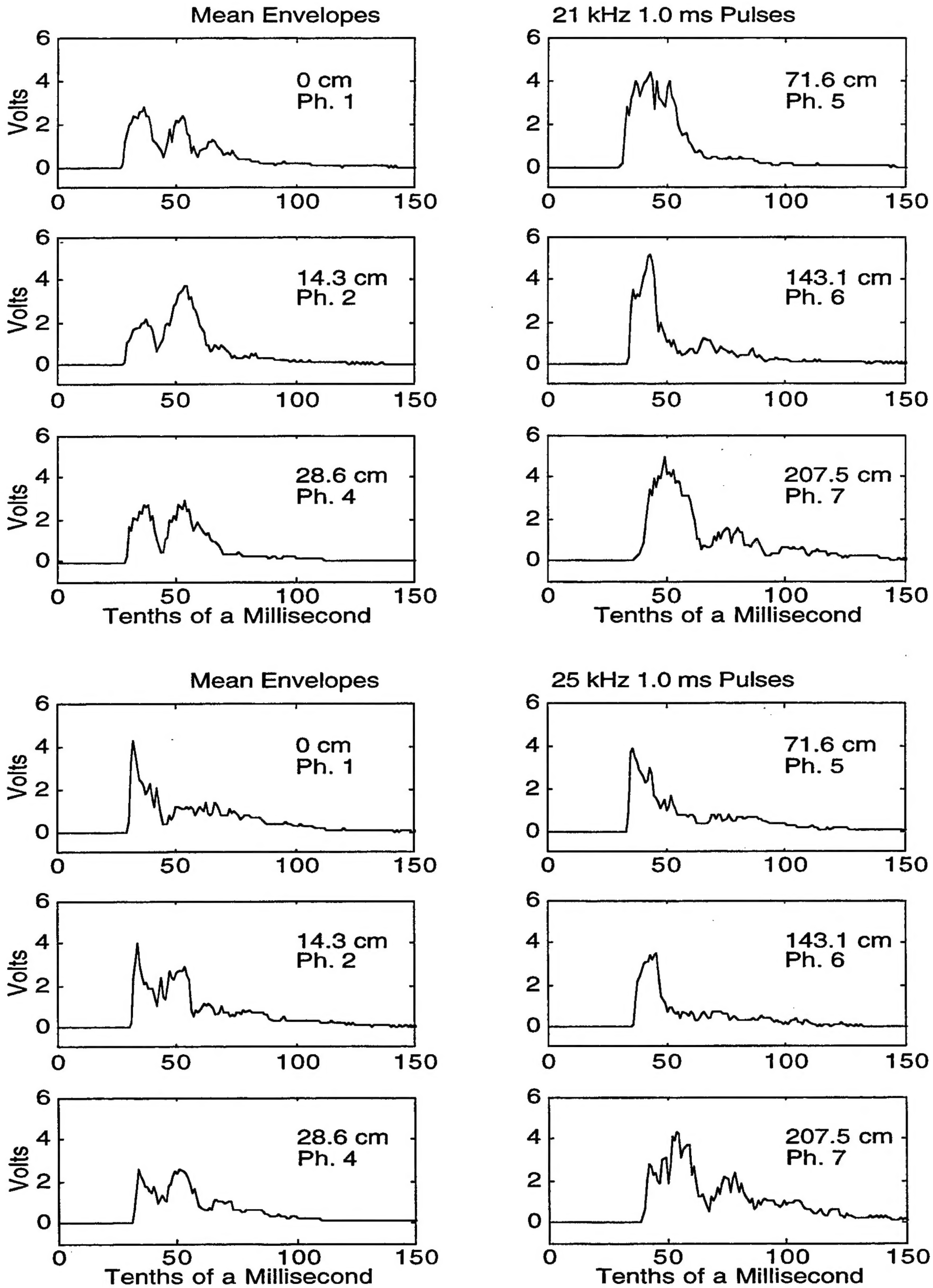

Figure 3. Mean of 128 envelopes at each depth for 21 and 25 kHz 1 ms pulses. Levels are not calibrated to show differences between hydrophones or frequencies.

The transmission loss was obtained by subtracting the level at the hydrophone just below the surface (Ph.2) from that of deeper hydrophones so that a negative value indicates the amount of loss and positive values indicate how much the level increased. Depths of hydrophones below the sediment surface were determined from differences in pulse arrival times for the 15 kHz, 0.5 ms pulse data. The compressional wave velocity in the sediment (mean: 1431 m/s, standard deviation: 5.34 m/s), measured in the laboratory from the upper 50 cm of core samples taken in the area [7], was used to convert the times to depths. The tenth of a millisecond sampling rate of the envelopes results in depth increments of 14.3 cm and corresponding precision of depths.

Large variability in the slope of the envelopes for hydrophone 3 made determining the arrival time for depth calculations and averaging over the pulse length difficult. Instead of being between hydrophones 2 and 4, it seemed to be deeper than hydrophone 7, as shown in Figure 1, for some frequencies and a little shallower for others. Therefore, hydrophone 3 data were not included in plots of levels vs. depth and frequency.

Results

In Figure 2, two gridded waterfall plots show the variability among pulses in representative data sets. They show very consistent arrival times within the 128 second runs. The plots in most runs were consistent, although some indicate a gradual change of one to two samples within two minutes (see Appendix A for additional examples). Figure 2A also shows consistent pulse amplitude, but for some runs, such as shown in Figure 2B, there were substantial changes. Small motions of the source suspended over the side of the research vessel and fluctuations in the water column are the most probable causes of these changes. Since we are

looking at differences between two hydrophones in the same run, however, these changes are not important.

A mean envelope for the 128 pulses in a run shows the average direct arrival and scattered returns from features in the sediment. The mean envelopes for runs 29 and 32 are shown in Figure 3. For hydrophones 1, 2 and 4, the direct arrival and primary scattered signals are separated by several samples (tenths of a millisecond). The direct arrival was stronger than the scattered signal in all cases for hydrophone 1. Eleven out of twelve cases for hydrophone 2 have stronger peak direct signals than peak scattered signals. For hydrophone 4, 3 out of 12 runs show

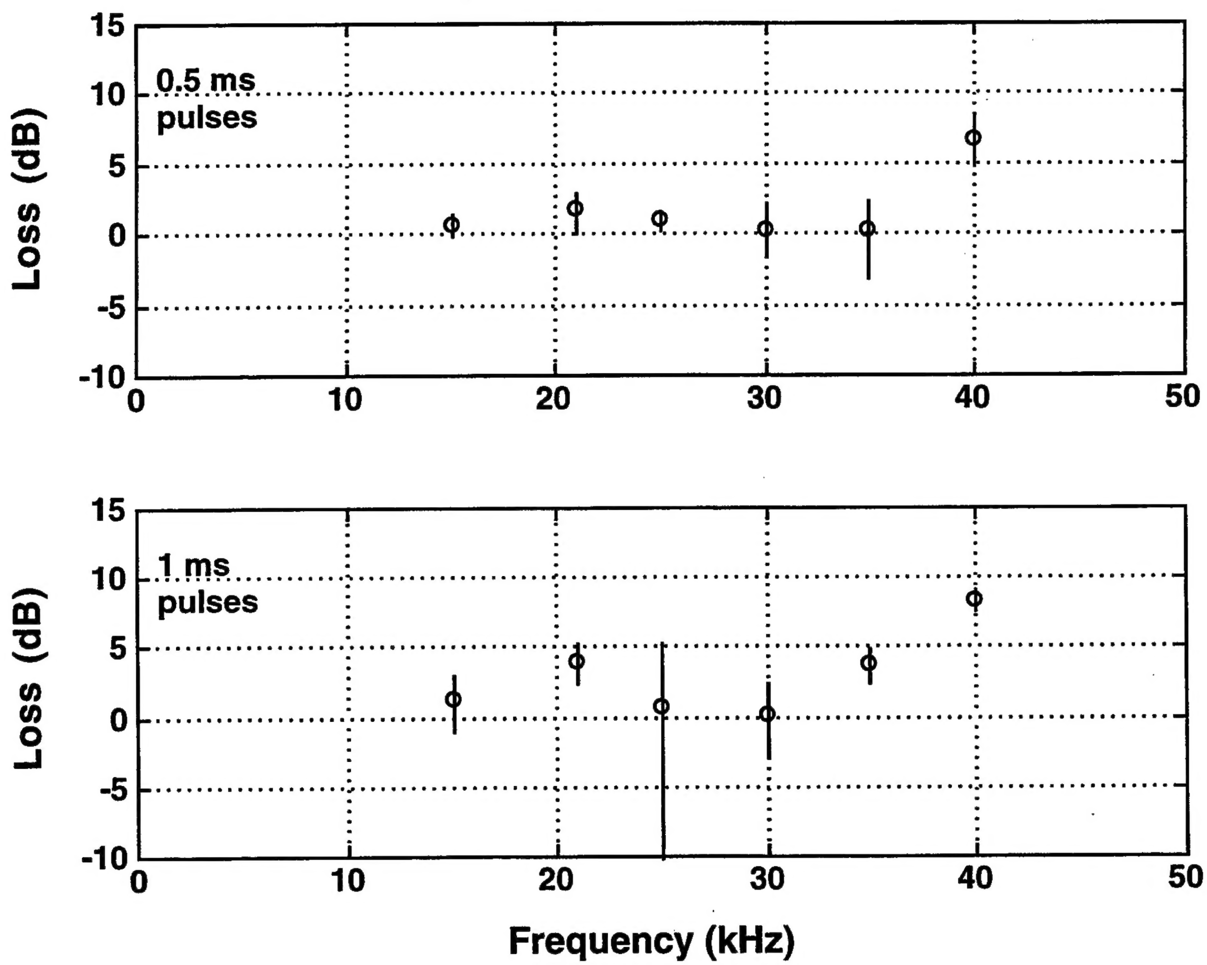

Figure 4. Means and standard deviations of insertion loss (Phone 1 - Phone 2) as a function of frequency.

stronger peak scattered signals than peak direct arrivals. For hydrophones 5, 6 and 7, the two arrivals overlap.

Insertion loss values are shown in Figure 4. The loss was less than 5 dB, except at 40 kHz. Since the soft mud at the bottom of Eckernförde Bay does not have a density much different from that of water, a large percentage of the 15 to 35 kHz signal energy can penetrate the water-sediment interface and very little is reflected back from the interface. Some mean loss values were higher for the longer pulse length , but standard deviations for the two pulse lengths overlapped. The 25 kHz, 1ms pulse length direct arrivals had a sharp peak, while the other frequencies did not. This sharp peak was responsible for the high standard deviation (see Figure 3).

Figure 5 shows the received levels relative to those of hydrophone 2 as a function of frequency for each depth. Figure 6 shows the same results plotted as a function of depth for each frequency. The results are similar for 0.5 and 1.0 ms pulses although there are a few wide variations. Levels at the 28.6, 71.6 and 143.1 cm depths were generally stronger than the level received at 14.3 cm, while the level at 207.5 cm was lower. Levels at the 143.1 cm depth increase with frequency from 15 to 35 kHz. Other depths do not seem to show a consistent pattern of frequency dependence, except that, for all depths, there is an increase in level between 15 and 21 kHz. The 15 kHz levels show a rapid decrease with depth. Levels for 21 kHz show a slight decrease with depth. For frequencies from 25 to 40 kHz, the 143.1 cm depth had higher levels than other depths.

Discussion

Insertion loss depends only on the amplitudes of the direct arrivals at hydrophones 1 and 2. This measurement shows that normal-incidence acoustic

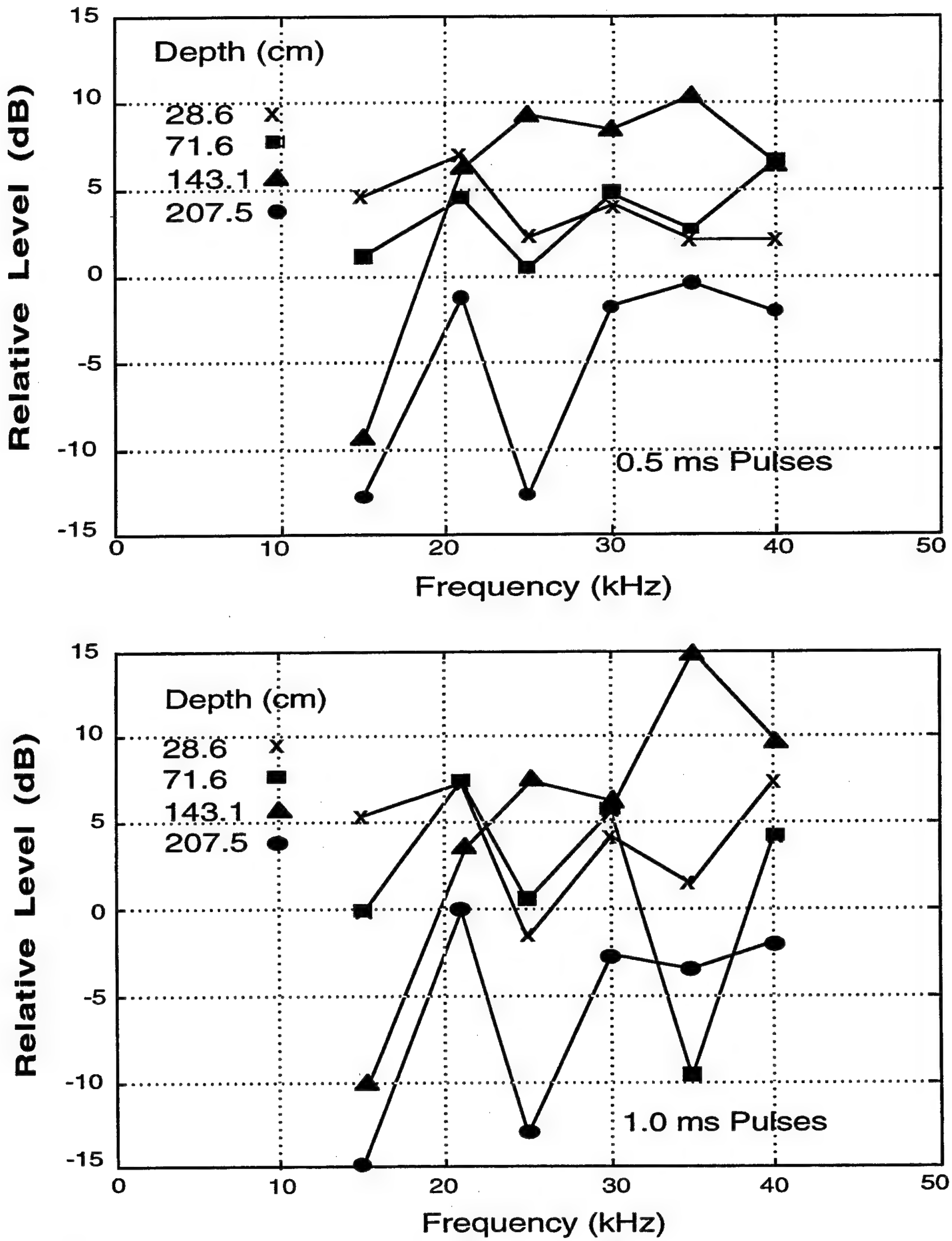

Figure 5. Received levels relative to hydrophone 2 (14.3 cm) versus frequency for each receiver depth.

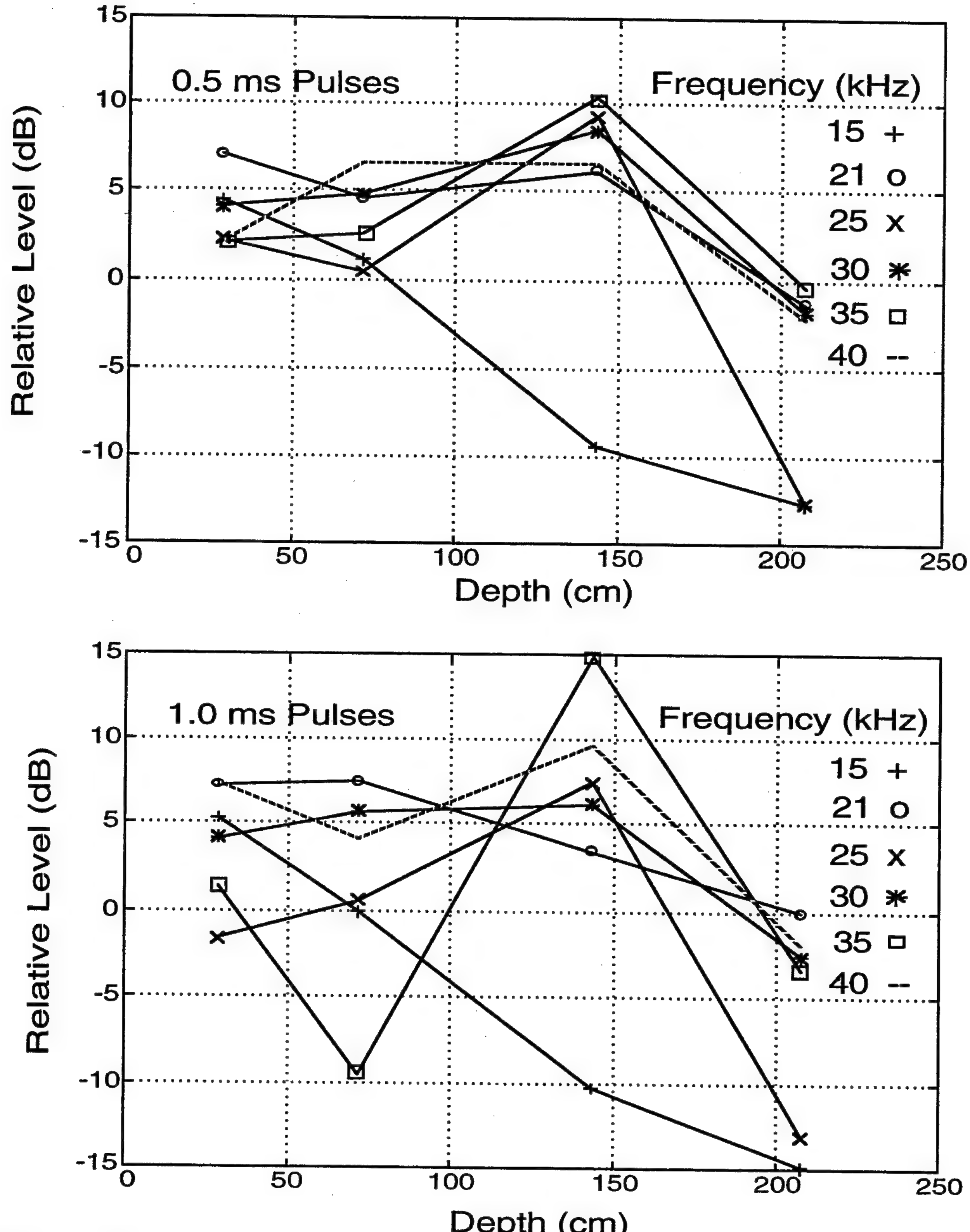

Figure 6. Received levels relative to hydrophone 2 (14.3 cm) versus receiver depth for each frequency.

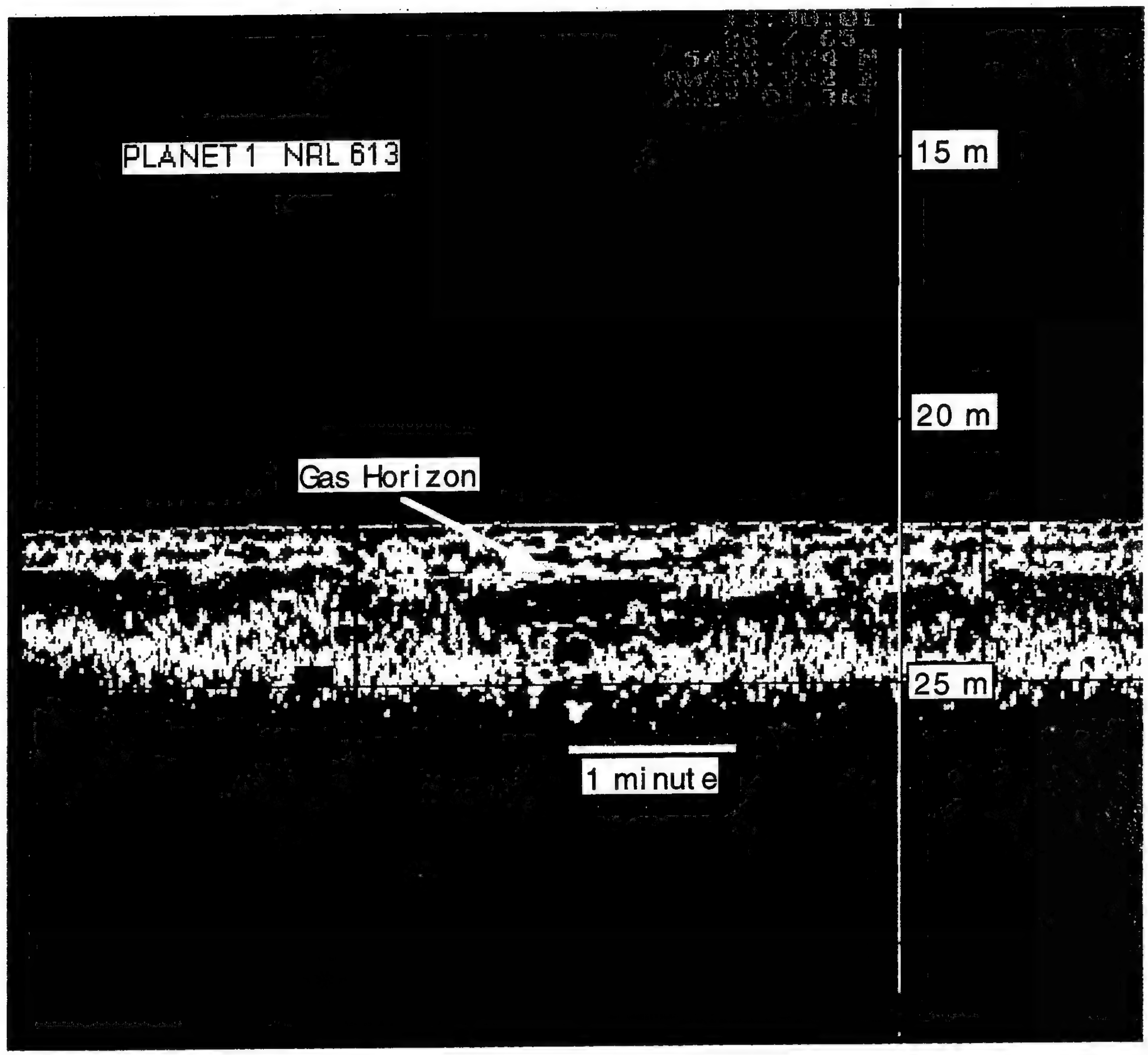

Figure 7. Acoustic Sediment Classification System data recorded at CBBL test site. Horizontal axis is elapsed time, as WFS PLANET was anchored while these data were collected. Notice how the gas horizon reflection changes in intensity and depth while the ship swung on its anchor over small distances. Depth below the air-water interface is shown beside the bright vertical line. The water-sediment interface is around 22 m. [10]

energy in the 15 to 35 kHz range can easily penetrate the mud bottom of Eckernförde Bay. The reason for the 6 to 9 dB insertion loss at 40 kHz is not known at this time, but similar dips in received levels at higher frequencies have been reported from other bottom penetration experiments. For example, an experiment near Panama City, Florida observed that sound pressure in the sediment at near-normal incidence decreased sharply to 25 dB below expected values for 60 kHz data at a site characterized as fine sand; a site with clay sediment had 6 dB lower values at 60 kHz than at 30 kHz.[9] A variable amount of scattering at 30 kHz at the sediment interface was observed in Eckernförde Bay, which was attributed to small bubbles trapped in the upper 2 cm of sediment.[6]

In a relatively homogeneous sediment, a steady decrease in received levels with depth, and very little scattering, would be expected. Figures 5 and 6 show that this is not the case in Eckernförde Bay, where the muddy bottom is a porous inhomogeneous medium in which various environmental processes control sediment structure. [10] Biological activity and consolidation produce a positive gradient in density and significant spatial variations in the upper 20 cm of sediment. The oxic zone is only 1 to 2 cm in depth, below which a black sediment with a hydrogen sulfide odor has been observed. [1] Sulfur bacteria metabolize organic matter and produce hydrogen sulfide to about 75 cm. Below that depth, methanogenic bacteria dominate and produce methane. [11] Bubbles are formed where methane concentrations exceed saturation limits. Methane gas rarely reaches the surface because the sulfur bacteria metabolize methane over 25 times faster than it is produced. [12]

Laboratory measurements of sediment core samples, maintained at in situ temperature and pressure, found an occasional bubble from 20 to 100 cm below the interface with many clusters of small bubbles deeper than 100 cm. [3,6] In addition subbottom seismic reflectivity profiles, like that in Figure 7, taken near the

experiment site in 1994 indicate a layer of gas bubbles, or gas horizon, between 70 and 120 cm below the sediment-water interface. The depth and intensity of the gas horizon changed within the 8.5 minutes of data shown in the Figure while the ship swung on its anchor over distances of only a few meters. [10] The data in Figure 7 were taken in water depths a few meters shallower than that where data for Figures 5 and 6 were collected, and the research vessel had not yet been 3-point moored. The 3-point mooring significantly reduced movement of the ship so that the gas horizon could be assumed to be constant during the high-frequency acoustic experiment.

When insonified by an acoustic pulse, gas bubbles in sediment exhibit dynamic resonance like that of gas bubbles in water. Well below the resonance frequency, the bubbles are small compared to acoustic wavelength and are ineffective scatterers. However, near and above resonance, bubbles are strong omnidirectional scatterers due to the large acoustic impedance difference between gas and mud. The bubbles in Eckernförde Bay during the CBBL experiment were reported to have radii between 0.3 and 5.0 mm. [6,10] The resonance frequency range at a depth of 24 m calculated for bubbles of this size distribution using the properties of Eckernförde Bay mud [10] in a model of scattering for bubbles in sediment [13,14] is between 1 and 25 kHz. Figure 8 shows the relationship between bubble radius and resonance frequency at 24 m in Eckernförde Bay mud and other substances. [10]

Figure 3 shows the direct arrival followed by scattered acoustic energy for each hydrophone. Two way travel time from hydrophone 2 to the sources of the second peak produces a bubble depth range of 114 to 243 cm below the water-sediment interface, using an average sound speed in mud of 1428 m/s. This is a maximum depth because it is possible that scattering is from out of plane sources as well as from directly below the receiver. The strongest part of the reverberation

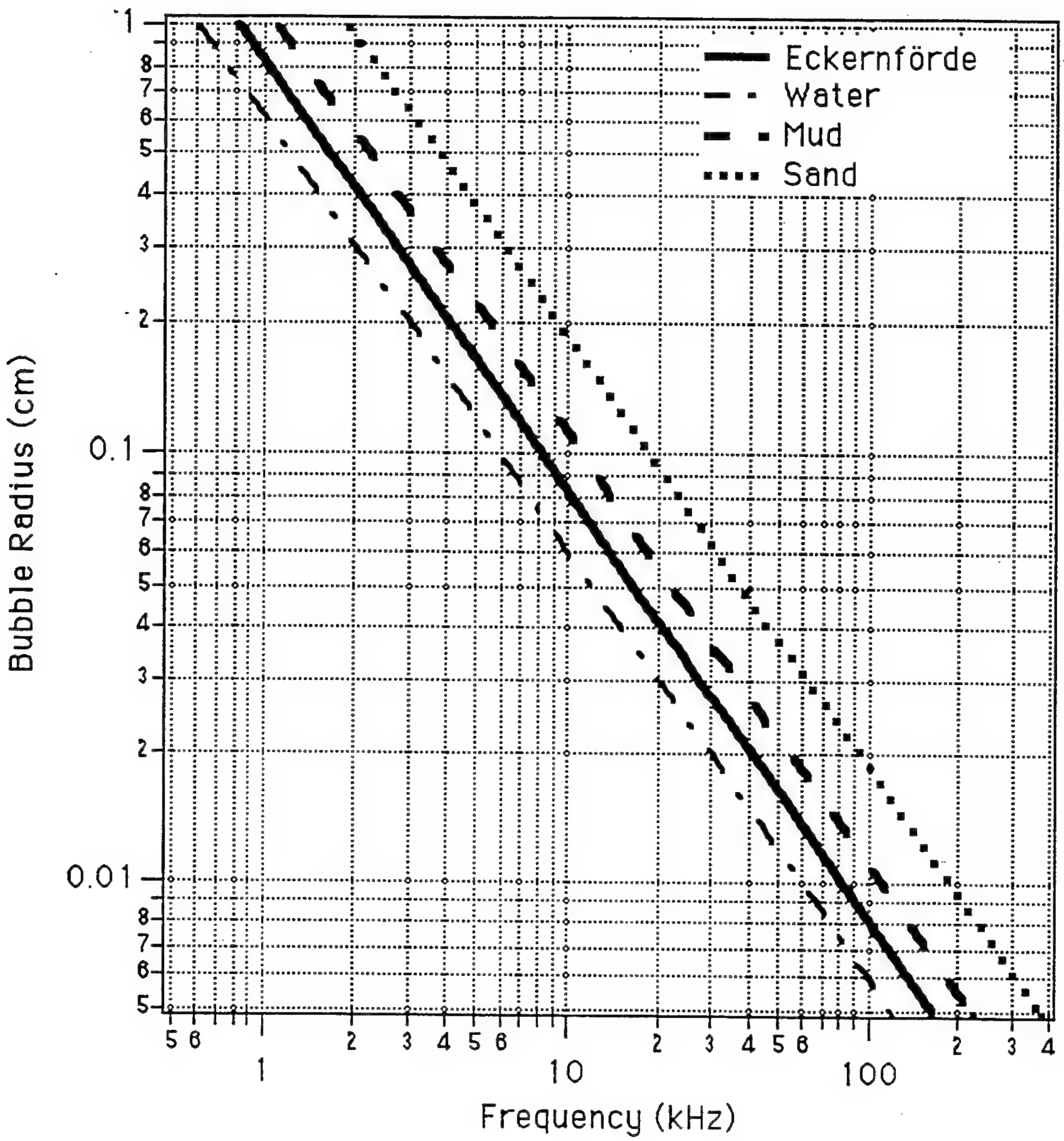

Figure 8. Gas bubble radius versus resonance frequency at 24 m depth for Eckernförde Bay sediments compared to other sediment types as well as seawater. [10]

peak occurs at a time which indicates depths up to 186 cm. It would be reasonable to deduce that the largest bubble population is around that depth or a little shallower. This corresponds to results shown in Figures 5 and 6 where most frequencies have higher levels at 143.1 cm.

At 28.6 cm depth, the direct path and the reverberation from individual bubbles just begin to overlap, even though the main bubble layer has not begun. The 1.0 and 0.5 ms pulse length received pulses may include reflected sound from up to 100 and 64 cm below the interface, respectively. Results shown in Figure 6 indicate that all frequencies are near or above the resonance frequency of these few bubbles. The 25 kHz 1 ms pulse length data were not affected, probably because peak levels dropped off so quickly after the first few points. At 71.6 cm, the peaks begin to merge and at 143.1 cm there is a single peak, as shown in Figure 3. The 143.1 cm phone shows a high initial amplitude and less reverberation after the direct arrival since it is within the bubble layer. Thus, the combination of backscattering from bubbles and the direct path signal, for all but the deepest hydrophone shown in Figure 6, yields a higher received level than the direct path signal at the 14.3 cm phone.

Figures 5 and 6 indicate that scattering affects received levels at all experimental frequencies (15 to 40 kHz). But the smallest measured bubbles resonate at 25 kHz. Thus, if resonance scattering from bubbles is affecting 30 to 40 kHz returns, bubbles smaller than 0.3 mm must be present. X-ray computed tomography (CT) scan measurements showed that some sediment cores from near the acoustic experimental site had about 10 bubbles with radii around 0.7 mm and over 1000 bubbles with radii near 0.42 mm, the lower limit of the CT scan measurements, and it was postulated that numerous smaller bubbles exist. [6] There was significant variability in bubble positions and sizes in cores taken near the

acoustic site. [6] These results indicate that bubbles with radii as small as 0.17 mm are most likely present and caused scattering at 30 to 40 kHz.

Results at 15 kHz are different from those at other frequencies. Figure 6 shows that levels for the 28.6 cm phone are about 5 dB greater than those of the 14.3 cm phone and decrease rapidly for deeper phones. Figure 5 shows that other frequencies, except 25 kHz for 1 ms pulses, have levels within 3 dB of the 15 kHz level for 28.6 cm. The combination of transmission loss and bubble effects at 71.6 cm results in 15 kHz levels near 0 dB. At 143.1 cm, 15 kHz levels are about -10 dB, while higher frequencies have high levels. Because larger bubbles resonate at lower frequencies, these data indicate that 0.7 mm bubbles, which resonate at 15 kHz, occur in sediment down to 100 cm, but not at or below 143.1 cm.

Details of the frequency dependence shown in Figure 5 may be explained by the depth vs. bubble size distribution. Levels increase when bubbles of the right size are near the hydrophone. Part of the energy near the resonance frequency is absorbed so that in the absence of more bubbles of that size, deeper hydrophones will show a lower level compared to one in the bubble layer. There may be more than one layer for some bubble sizes. Received levels in Figures 5 and 6 range from -15 dB to +15 dB. Differences between the two pulse lengths are probably due to greater insonified volume for 1.0 ms pulse length data.

Conclusion

Acoustic amplitude fluctuations over 128 second intervals for various frequencies and hydrophone depths probably result from significant small scale spatial inhomogeneities in the water and sediment of Eckernförde Bay and small movements of the source. Most received pulse starting times indicated stable source-receiver geometry because they did not change by more than 0.1 ms (14.3

cm) within the 128 sample set recorded. Insertion losses were less than 5 dB except at 40 kHz where they were between 6 and 9 dB. The very low values obtained for insertion loss indicate that there was little acoustic attenuation between the hydrophone on the bottom and the one 14.3 cm below the water-sediment interface for frequencies from 15 to 35 kHz.

Received levels for different hydrophones, frequencies and pulse lengths had a 30 dB range. The data from the hydrophone just below the water-sediment interface was in the center of this range. Layers in the sediment, especially more than 70 cm below the surface, contained gas bubbles with resonant frequencies within the range of acoustic frequencies used. These caused the signal levels at hydrophones in the bubble layer to be higher than the signal level just below the sediment surface. Frequency and depth dependence of this data set suggests that, at this site, 0.7 mm and larger bubbles occur within 100 cm of the water-sediment interface while smaller bubbles, including some too small to be measured with CT scans, are concentrated near 140 cm depth in the sediment.

Acknowledgments

This work was sponsored by the Office of Naval Research with technical management provided by the Naval Research Laboratory. The author wishes to thank S. Stanic, the principal investigator, and those who participated with him in collecting data on this experiment. Special thanks are also due to R.H. Love for his thorough review of the report and many helpful recommendations, and to M.D. Richardson for providing valuable technical discussions, references from numerous CBBL participants, and Figures 7 and 8 from Reference 10.

References

1. Richardson, M.D., "Investigating the Coastal Benthic Boundary Layer," Eos, Transactions, American Geophysical Union, **75**, No.17,April 26, 1994, pp 201, 205, and 206.

2. Stanic, S., "Measurements of normal-incidence acoustic energy penetration in the soft sediments of Eckernförde Bucht, Germany," Internal report of experiment plan, 1994.

3. Richardson, M.D., and W.R. Bryant, "Benthic boundary layer processes in coastal environments: an introduction," Geo-Marine Letters **16** No.3 pp196-203, 1996.

4. Orsi, T.H., F. Werner, D. Milkert, A.L. Anderson, and W.R. Bryant, "Environmental Overview of Eckernförde Bay, Northern Germany," Geo-Marine Letters **16** No.3 pp140-147, 1996.

5. Bussman, I., and E. Suess, "Groundwater seepage in Eckernförde Bay (Western Baltic Sea): Effect on methane and salinity distribution of the water column," Continental Shelf Research (Special issue on CBBL projects, in press)

6. Anderson, A. L., F. Abegg, J. A. Hawkins and M. E. Duncan, "Bubble populations and acoustic interaction with the gassy seafloor," Continental Shelf Research (Special issue on CBBL projects, in press)

7. Richardson, M.D., and K. B. Briggs, "In-Situ and Laboratory Geoacoustic Measurements in Soft Mud and Hard-Packed Sand Sediments: Implications for High-Frequency Acoustic Propagation and Scattering," Geo-Marine Letters **16** No.3 pp196-203, 1996.

8. Wever, T. F. , F. Abegg, H. M. Fiedler, G. Fechner and I. H. Stender. "Shallow gas in the muddy sediments of Eckernförde Bay." Continental Shelf Research (Special issue on CBBL projects, in press)

9. Chotiros, N. P., "High frequency bottom penetration: Panama City experiment," ARL-TR-89-36, Final report under contract N00024-86-C-6134 Task 1, Project 17, Applied Research Laboratories, The University of Texas at Austin, 5 July 1989.

10. Wilkens, R. H. and M. D. Richardson, "The influence of gas bubbles on sediment acoustic properties: in situ, laboratory, and theoretical results from

Eckernförde Bay, Baltic Sea, Germany," Continental Shelf Research (Special issue on CBBL projects, in press)

11. Albert, D. B., C. S. Martens and M. J. Alperin, "Biogeo-chemical processes controlling methane in gassy coastal sediments 2. Groundwater flow control of acoustic turbidity in Eckernförde Bay sediments," Continental Shelf Research (Special issue on CBBL projects, in press)

12. Whiticar M. J., "The presence of methane bubbles in the acoustically turbid sediments of Eckernförde Bay, Baltic Sea. In: Fanning, K.A. and Manheim, F.T. (eds.), *The Dynamic Environment of the Ocean Floor.* Lexington, Massachusetts: Lexington Books. 1982, pp 219-235.

13. Anderson, A. L. and L. D. Hampton, "Acoustics of gas-bearing sediments I. Background," *Journal Acoustical Society America* 67, 1980, pp1865-1889.

14. Anderson, A. L. and L. D. Hampton, "Acoustics of gas-bearing sediments I. Background," *Journal Acoustical Society America* 67, 1980, pp1890-1903.

Appendix A

Waterfall Envelope Plots

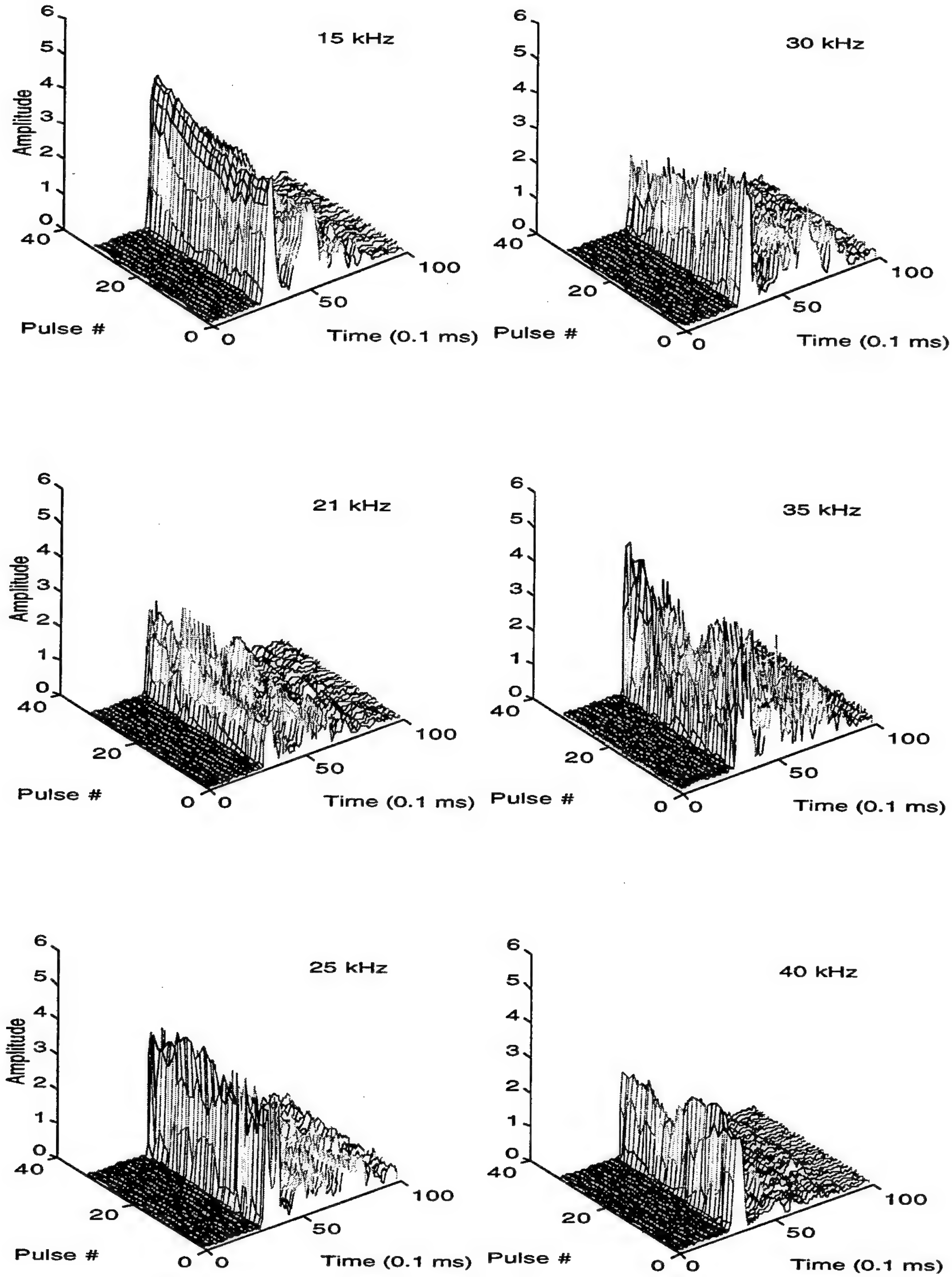

Figure A1. Waterfall envelope plots of 0.5 ms pulses from phone 1.

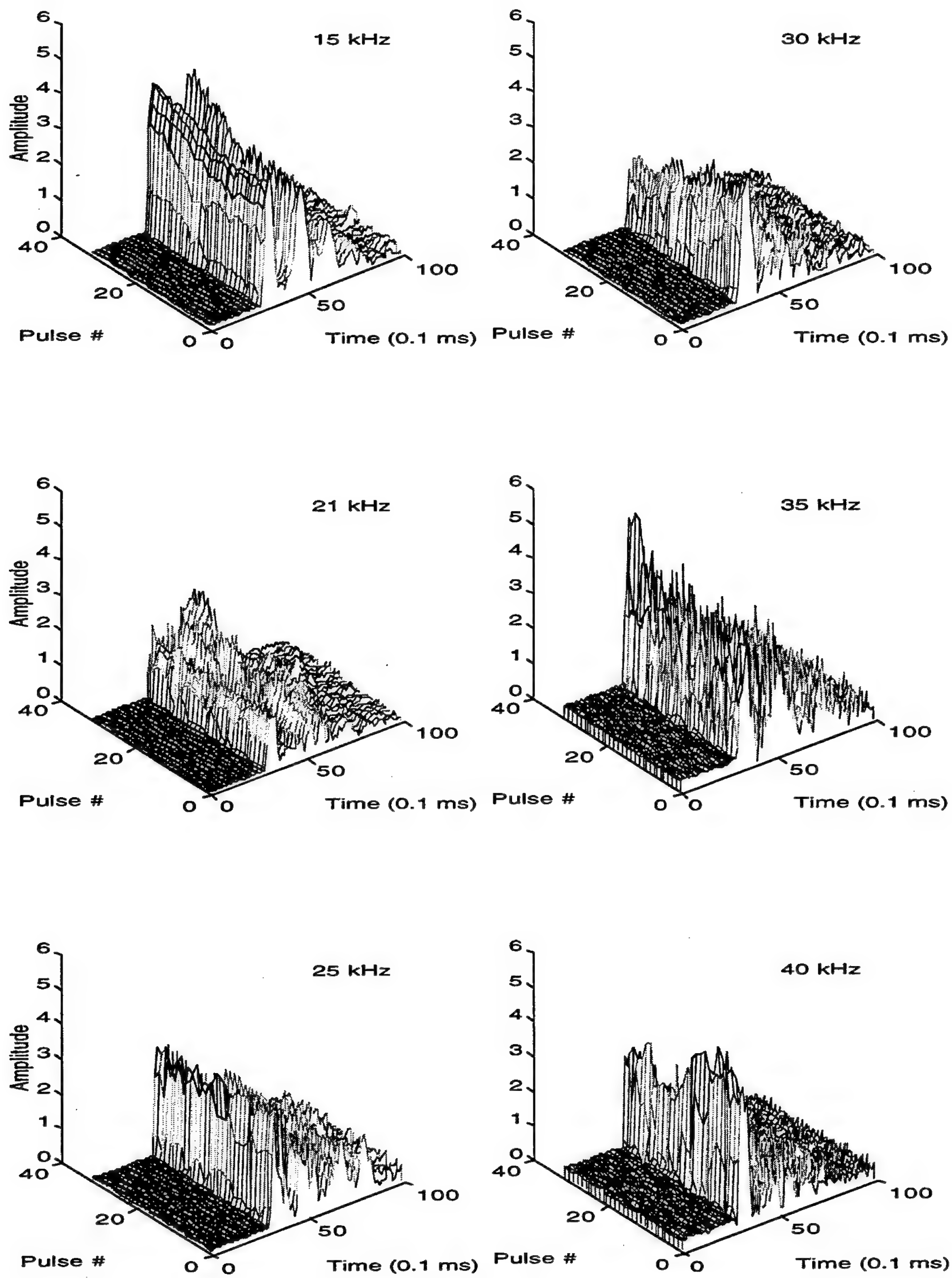

Figure A2. Waterfall envelope plots of 0.5 ms pulses from phone 2.

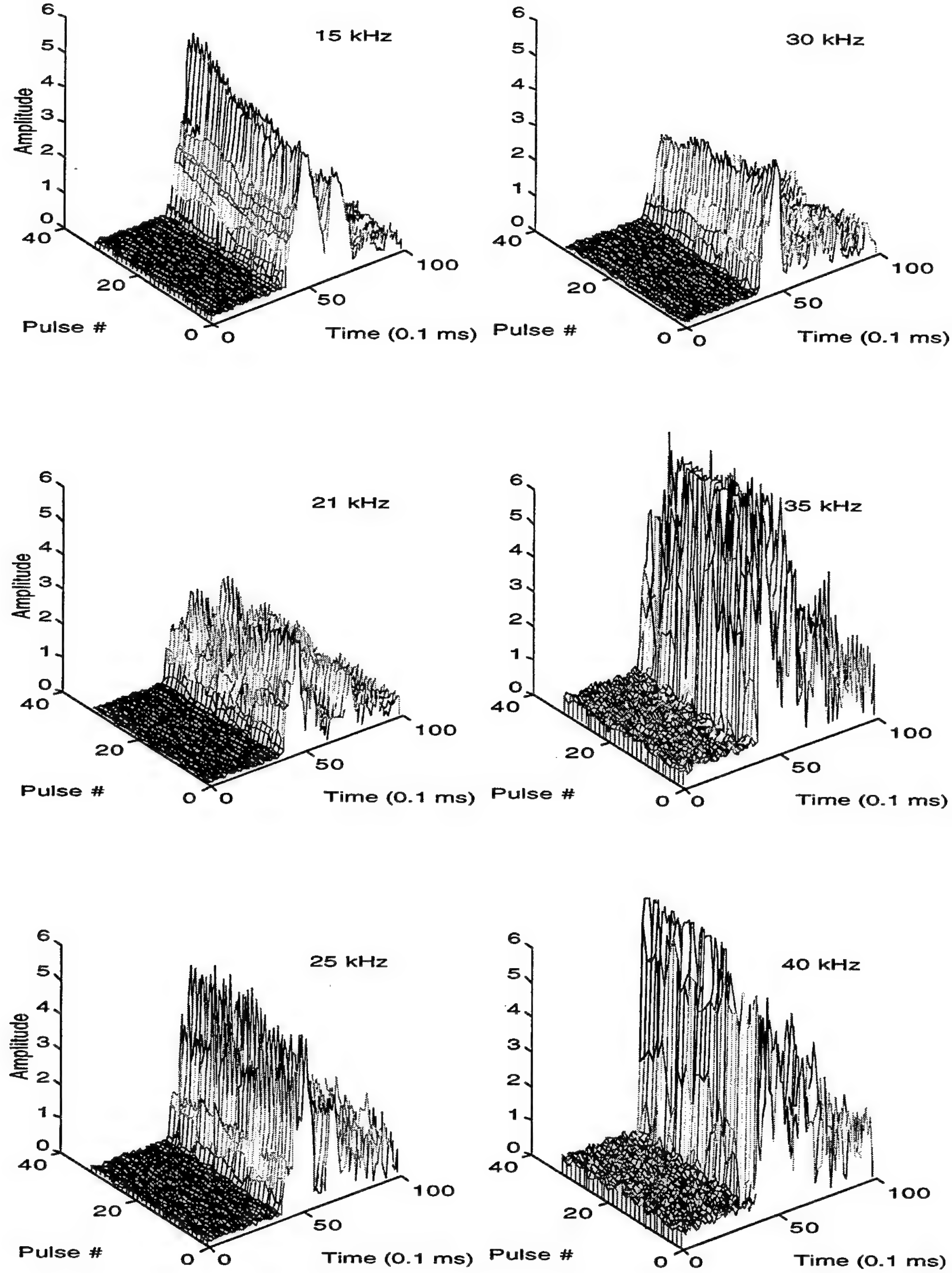

Figure A3. Waterfall envelope plots of 0.5 ms pulses from phone 3.

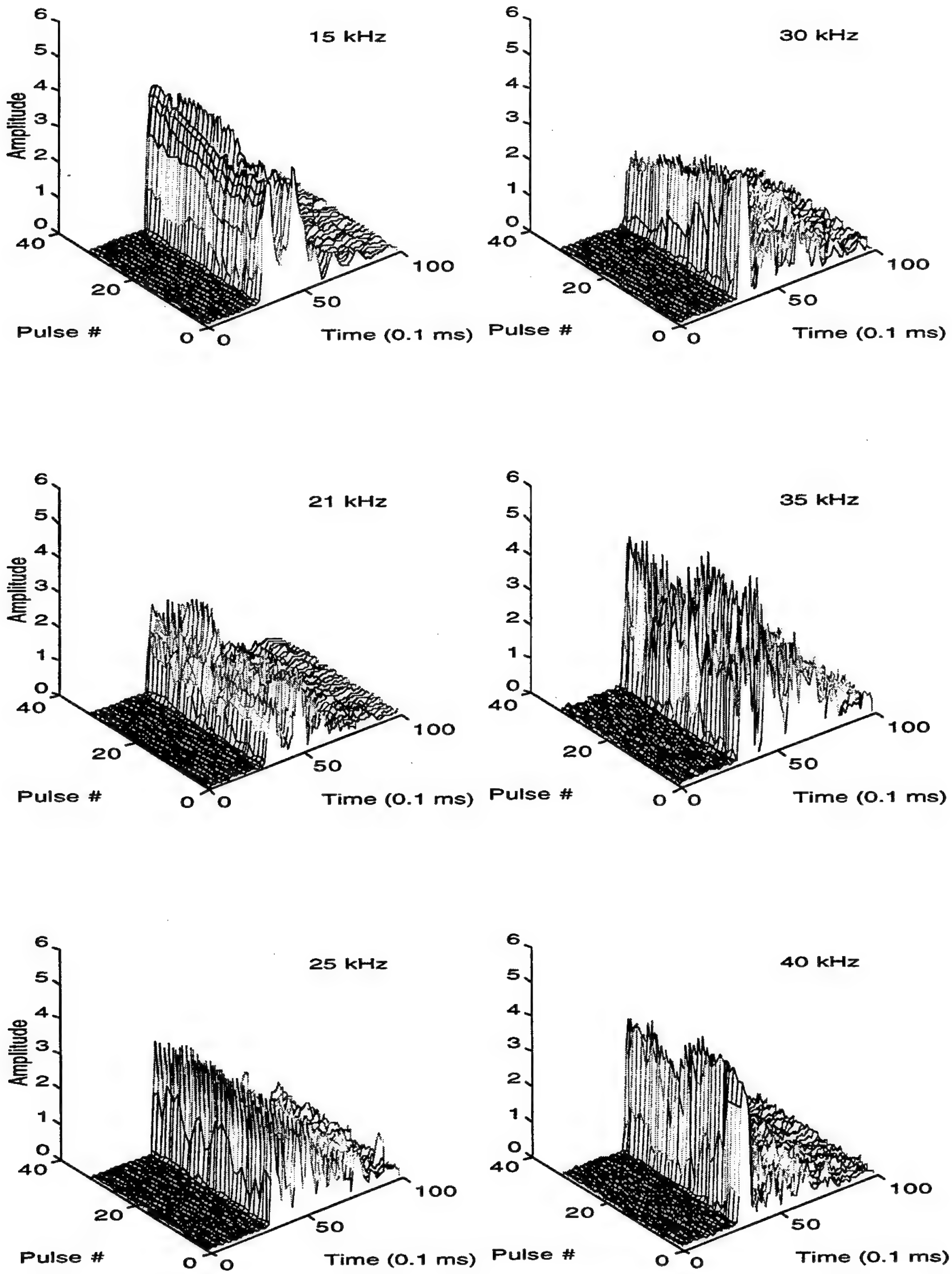

Figure A4. Waterfall envelope plots of 0.5 ms pulses from phone 4.

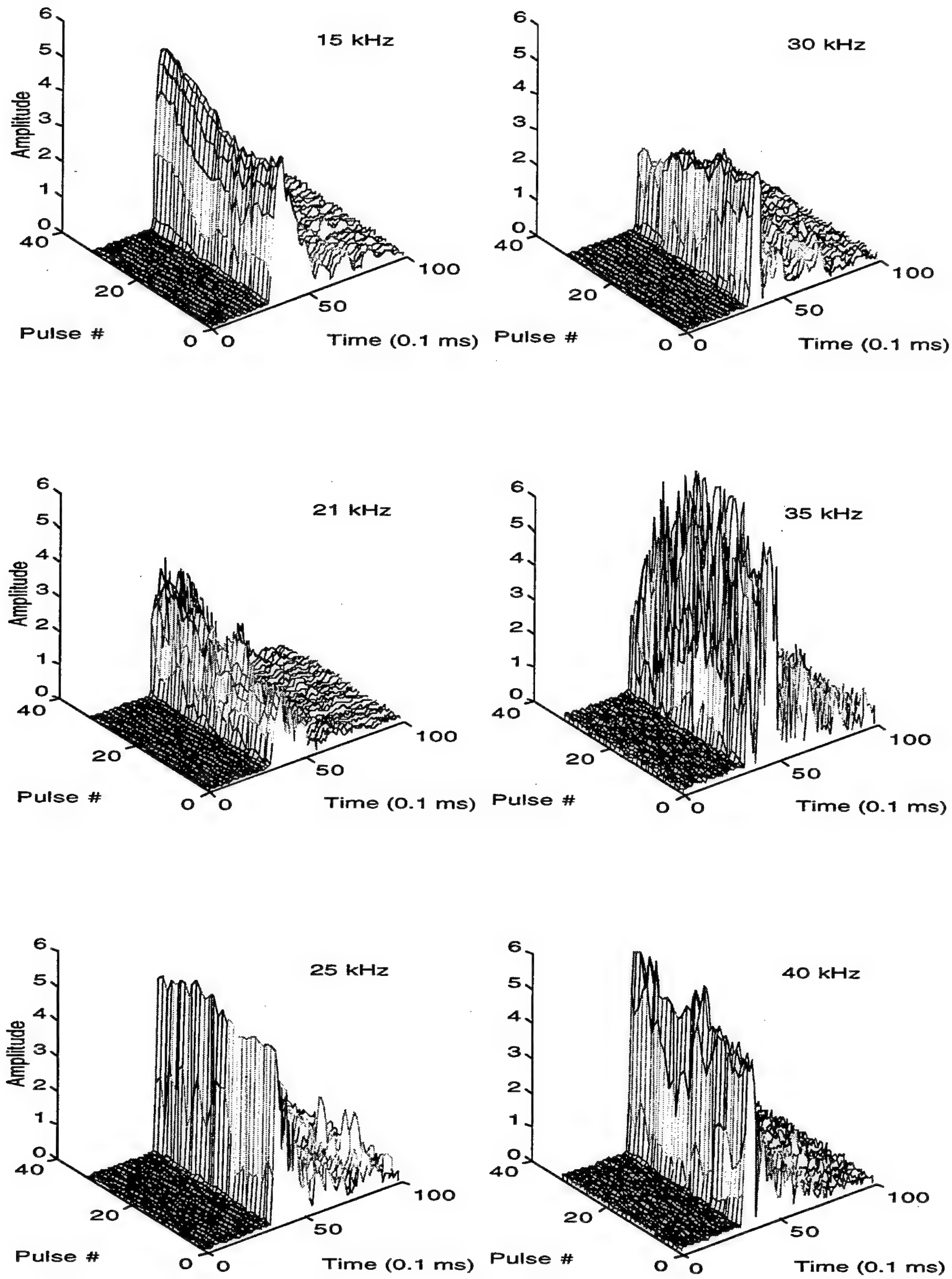

Figure A5. Waterfall envelope plots of 0.5 ms pulses from phone 5.

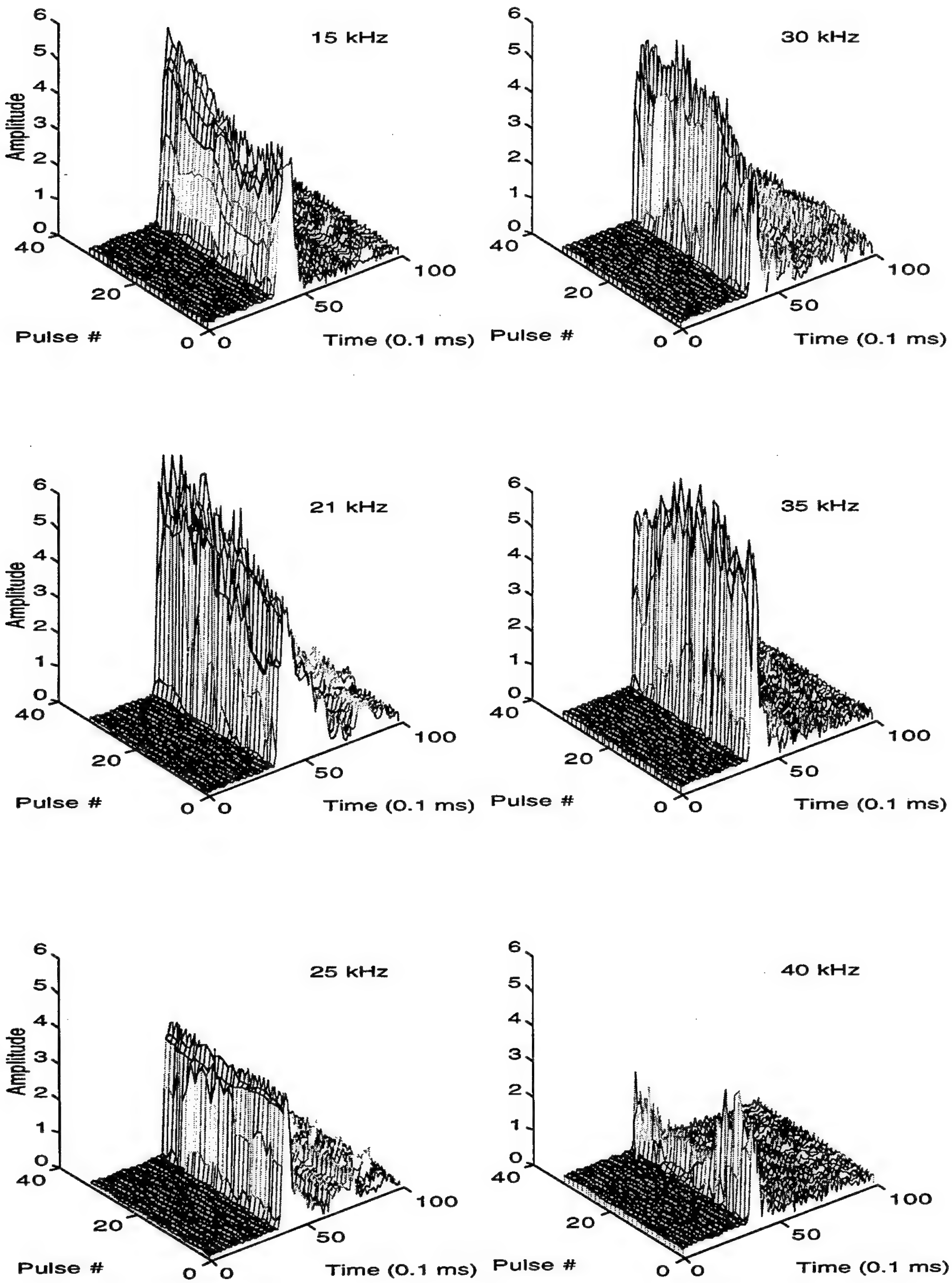

Figure A6. Waterfall envelope plots of 0.5 ms pulses from phone 6.

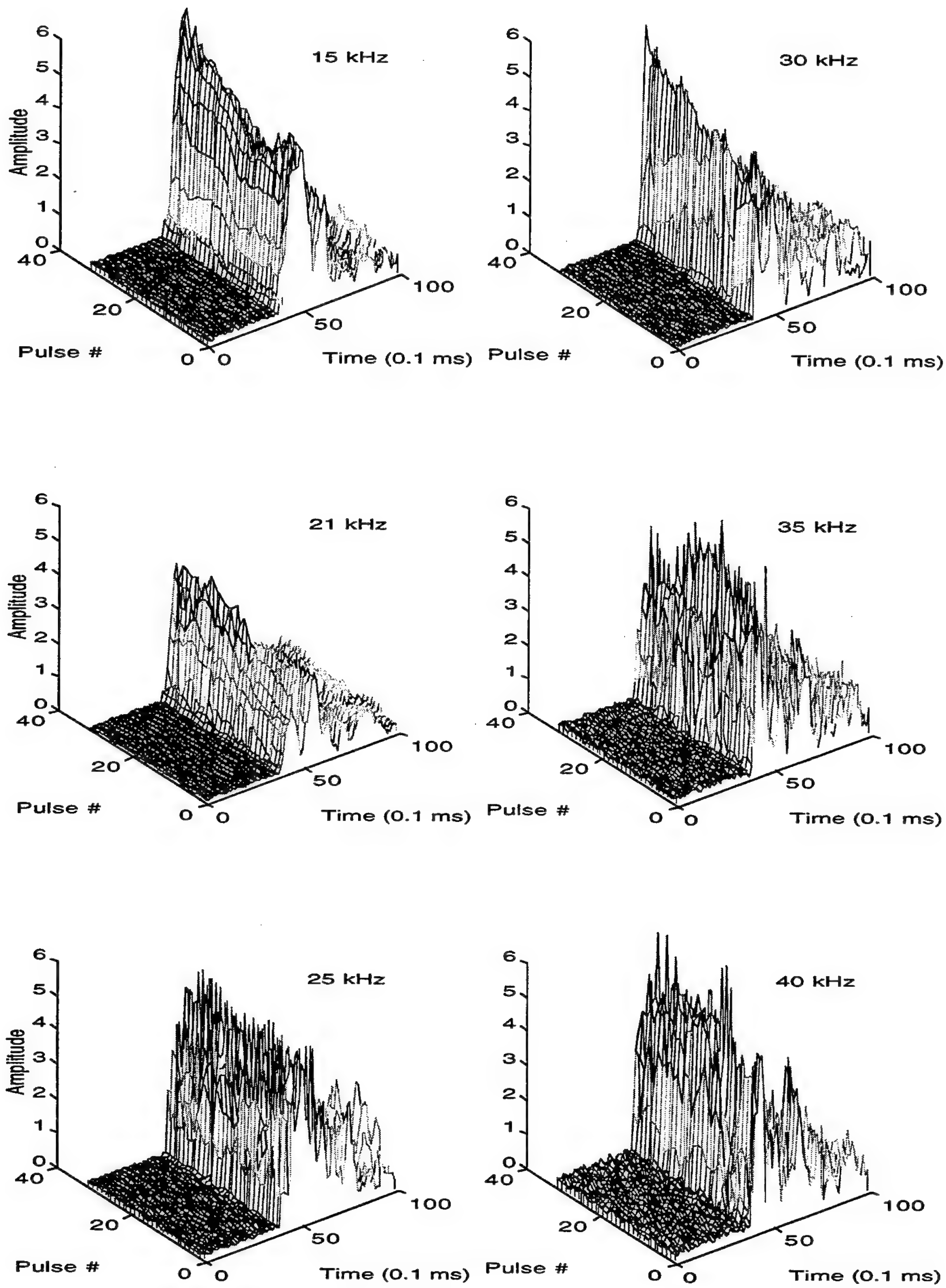

Figure A7. Waterfall envelope plots of 0.5 ms pulses from phone 7.

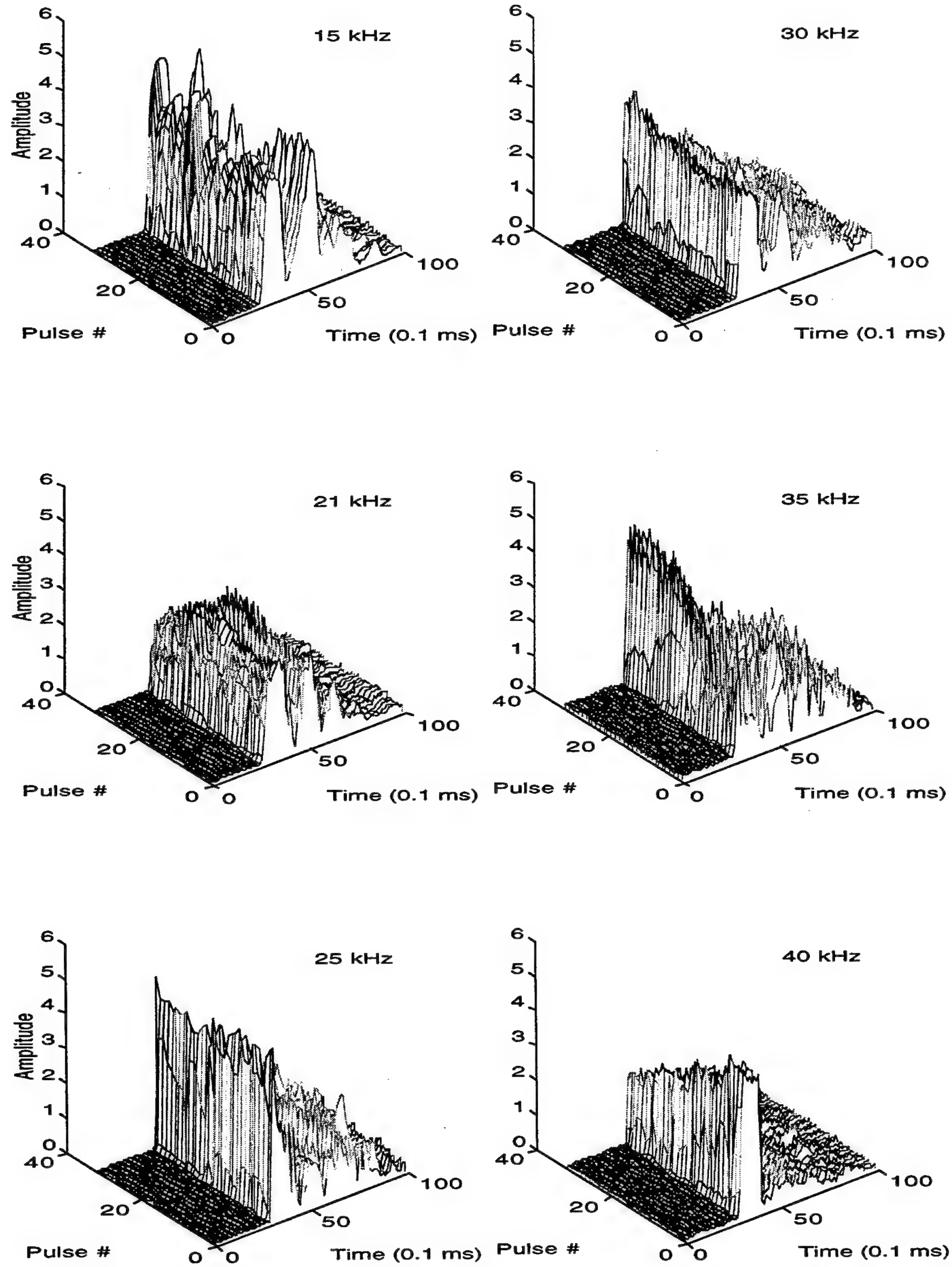

Figure A8. Waterfall envelope plots of 1.0 ms pulses from phone 1 .

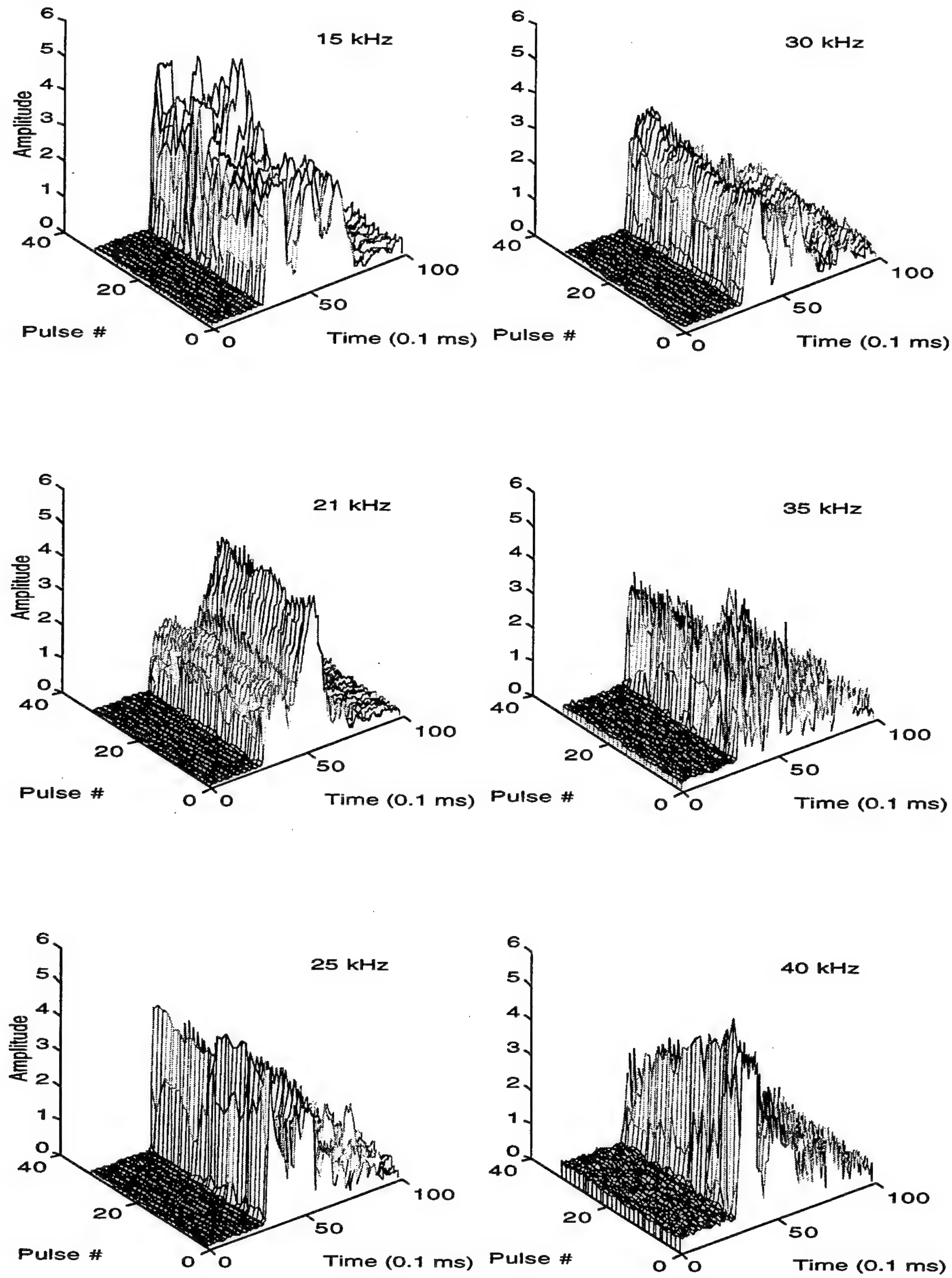

Figure A9. Waterfall envelope plots of 1.0 ms pulses from phone 2.

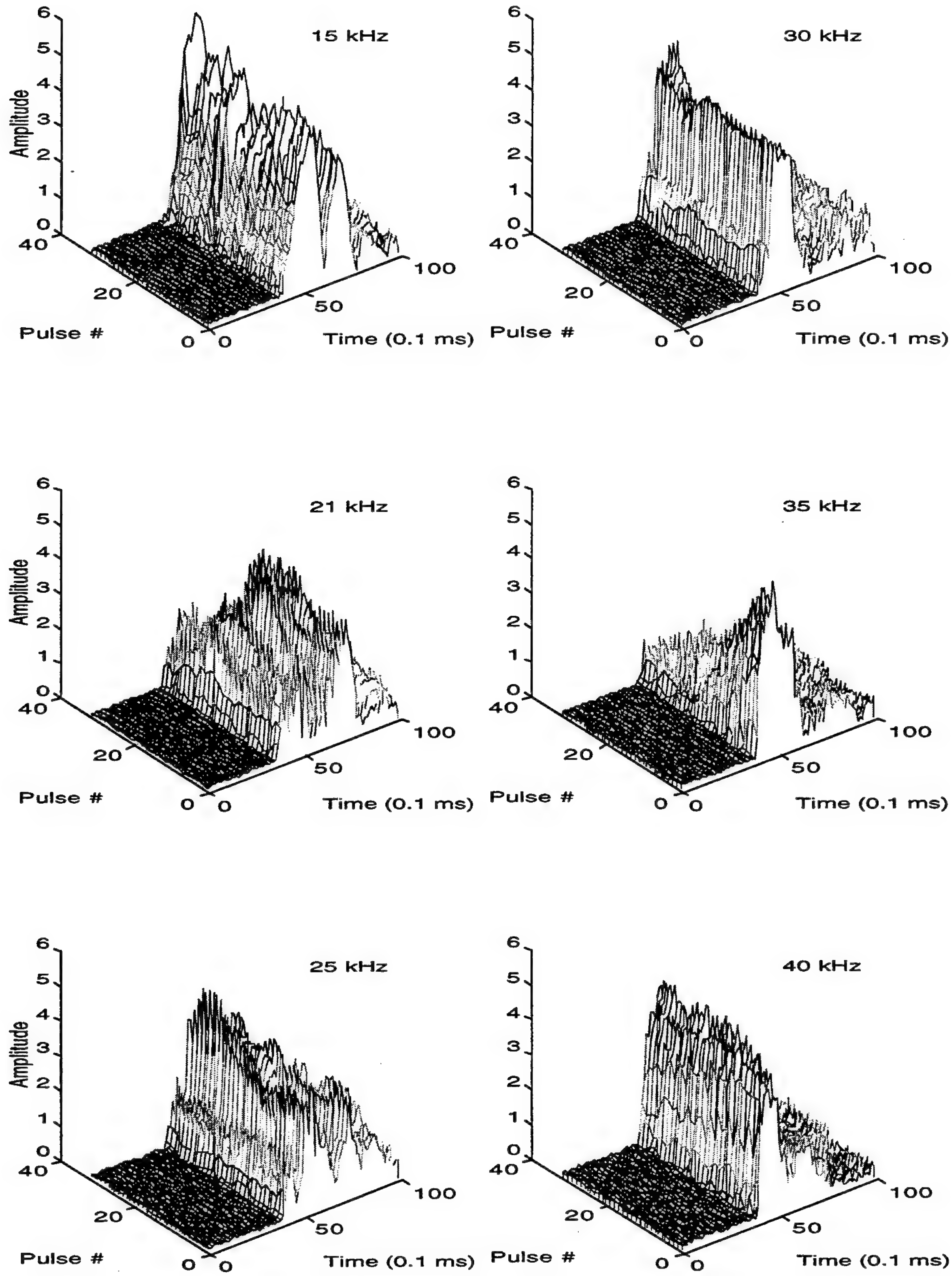

Figure A10. Waterfall envelope plots of 1.0 ms pulses from phone 3

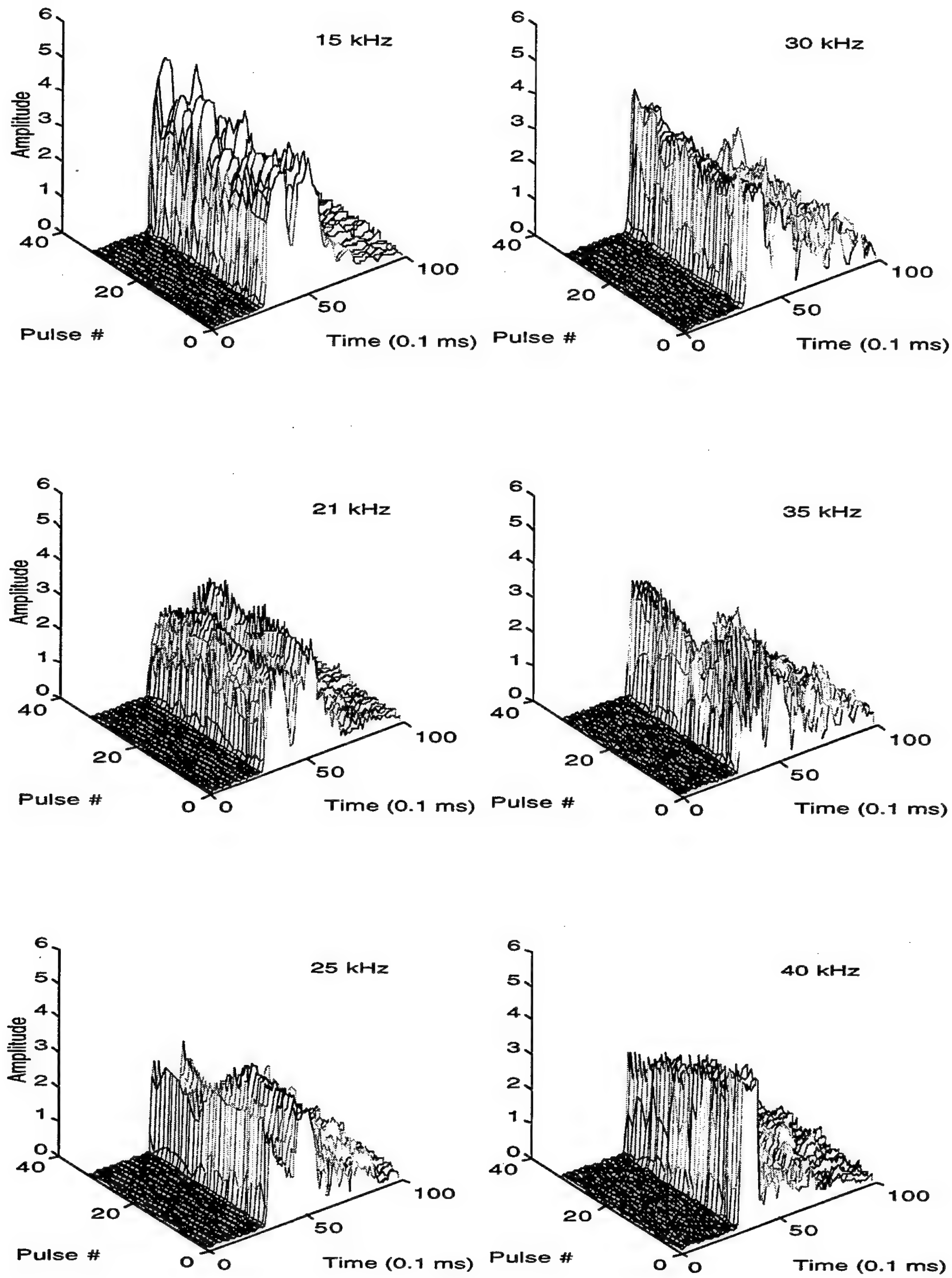

Figure A11. Waterfall envelope plots of 1.0 ms pulses from phone 4.

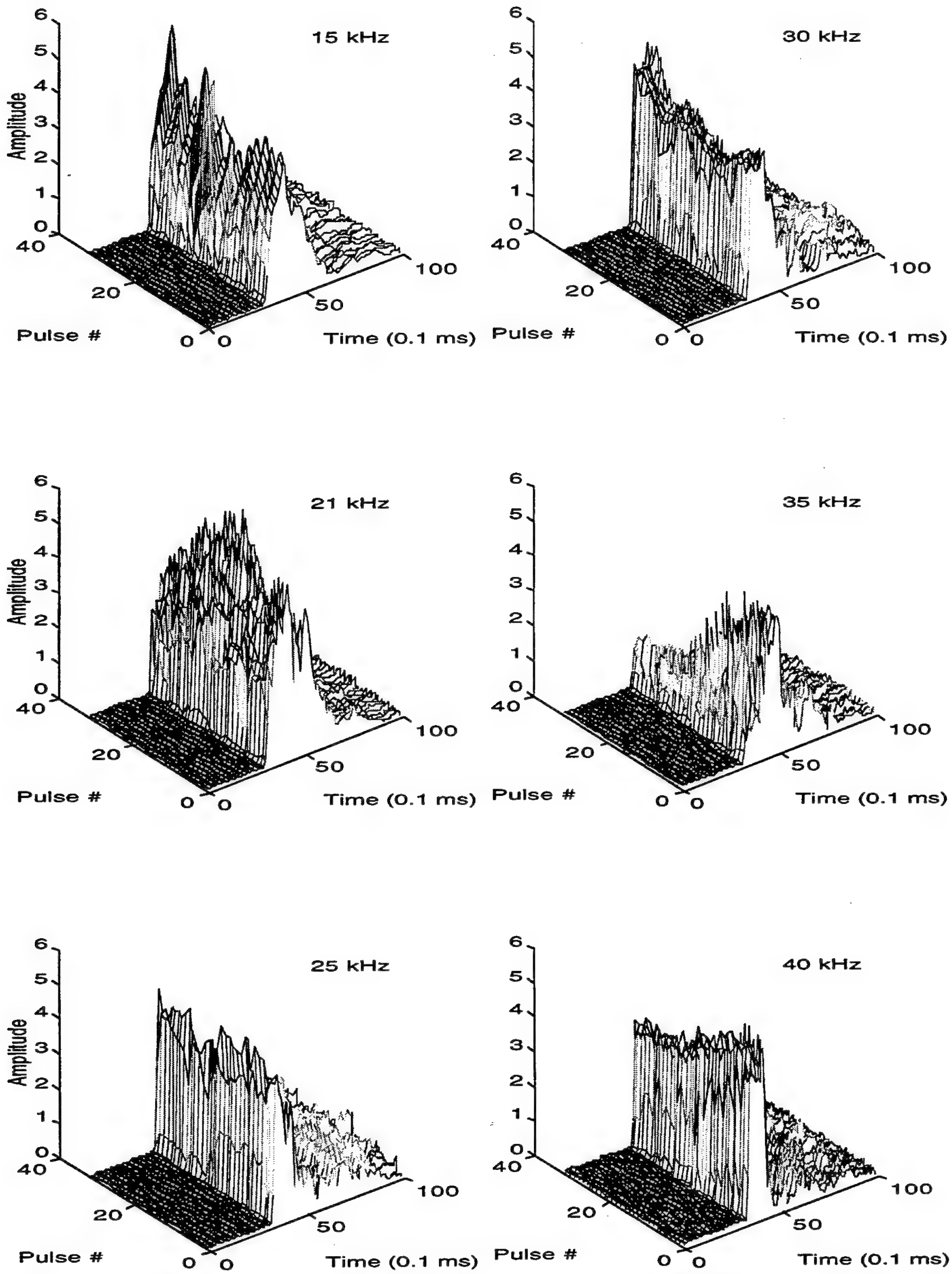

Figure A12. Waterfall envelope plots of 1.0 ms pulses from phone 5.

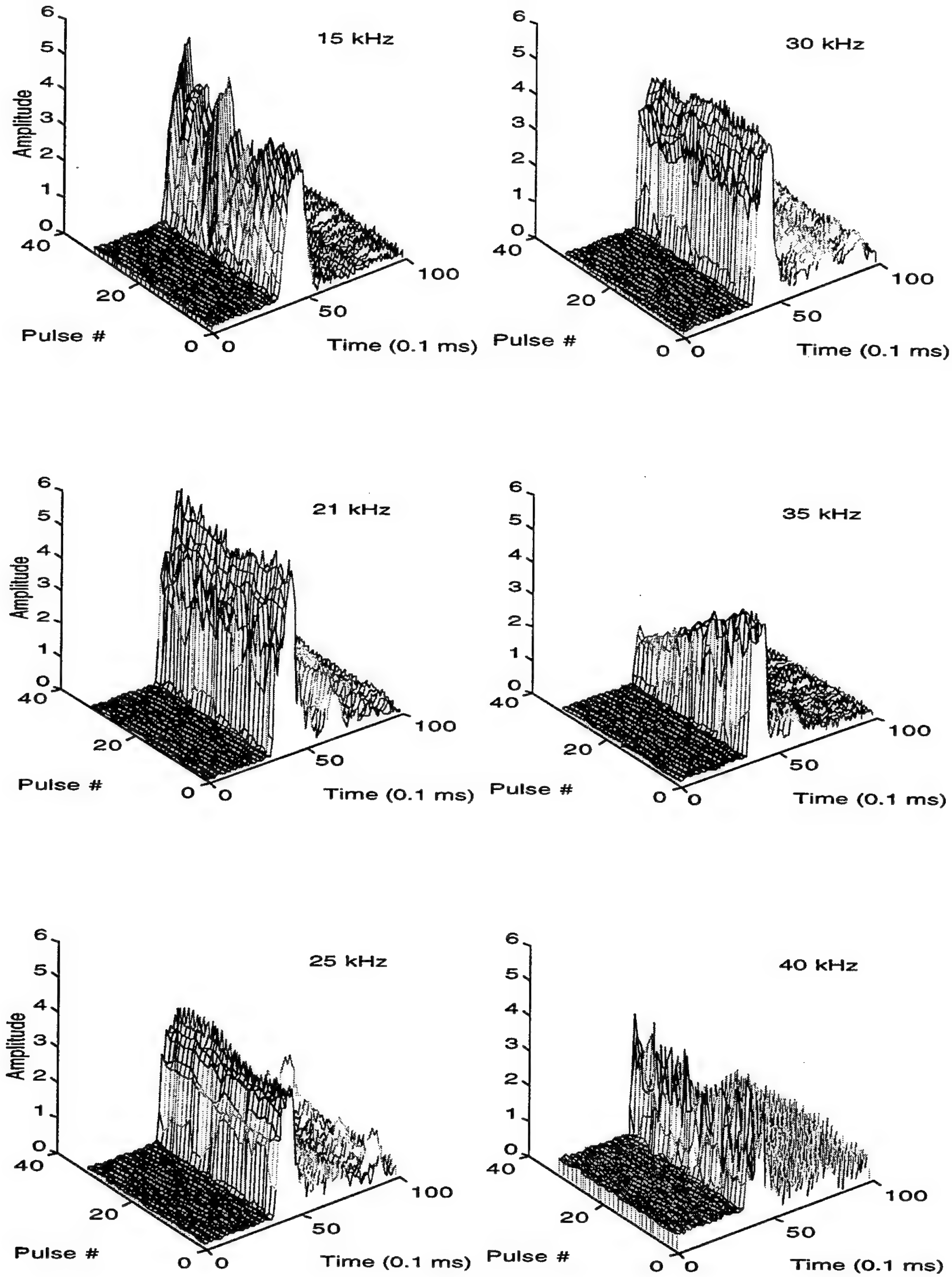

Figure A13. Waterfall envelope plots of 1.0 ms pulses from phone 6.

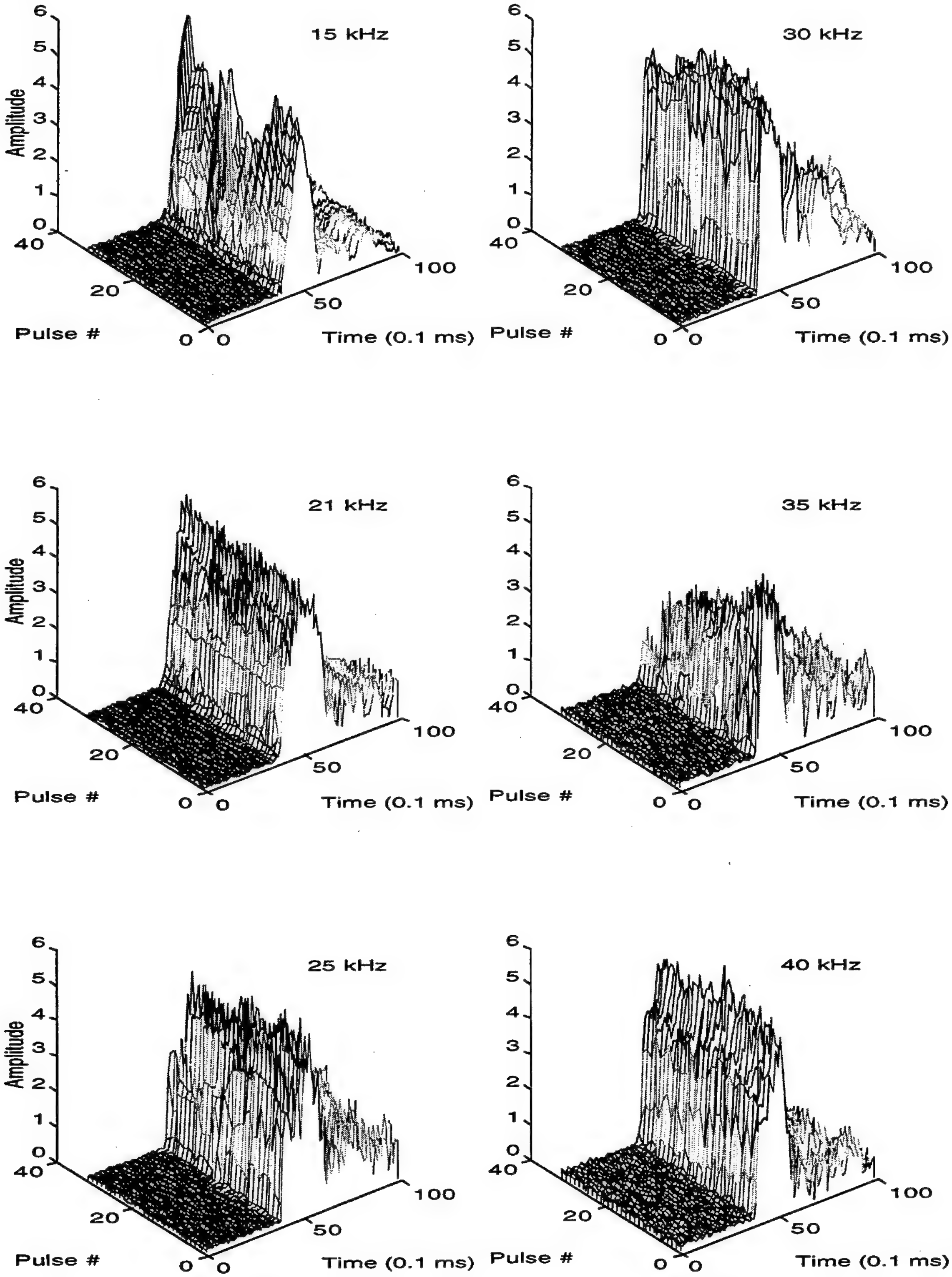

Figure A14. Waterfall envelope plots of 1.0 ms pulses from phone 7.

Appendix B

Mean Envelopes

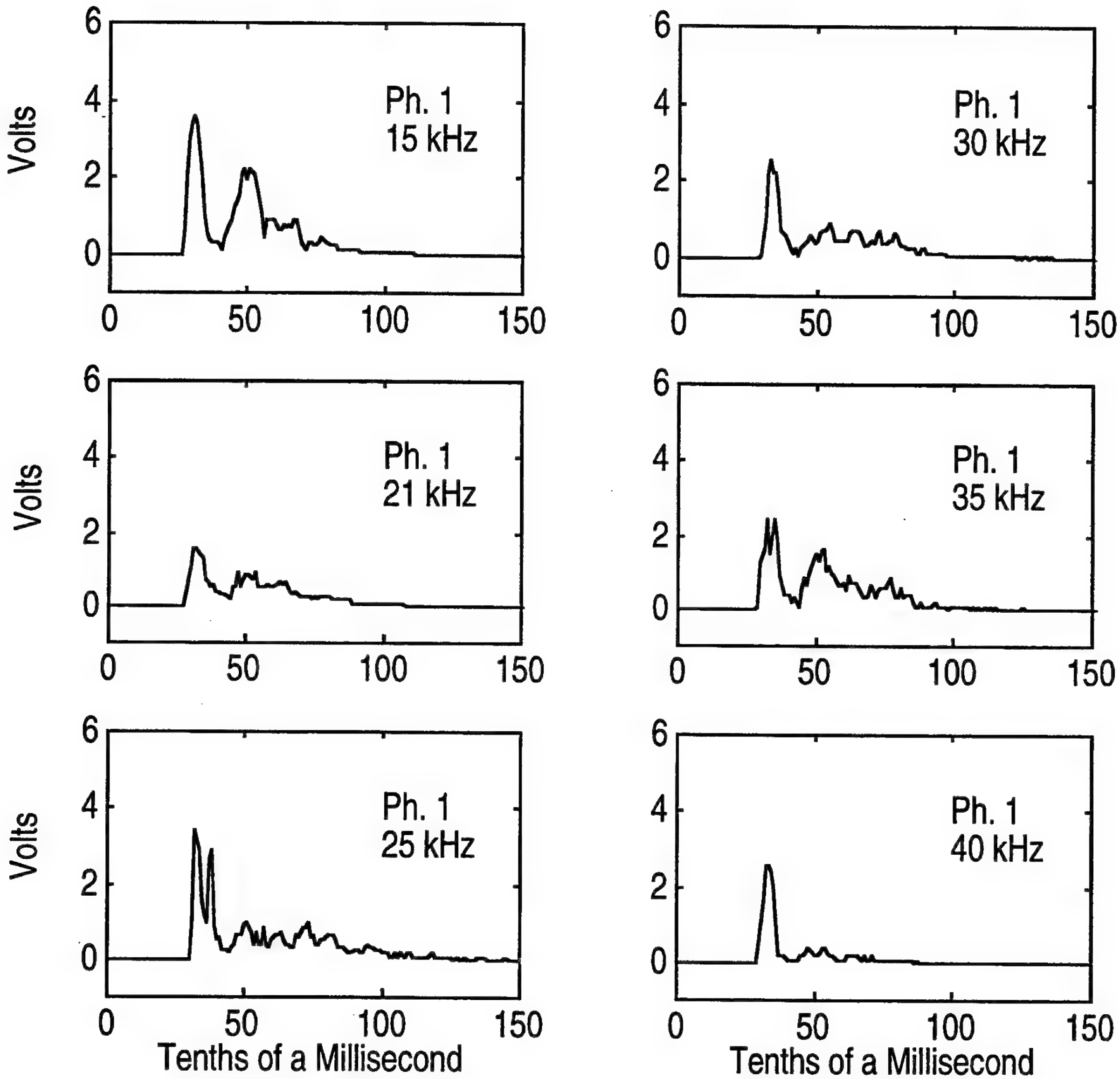

Figure B1. Phone 1 mean envelopes of 0.5 ms pulses.

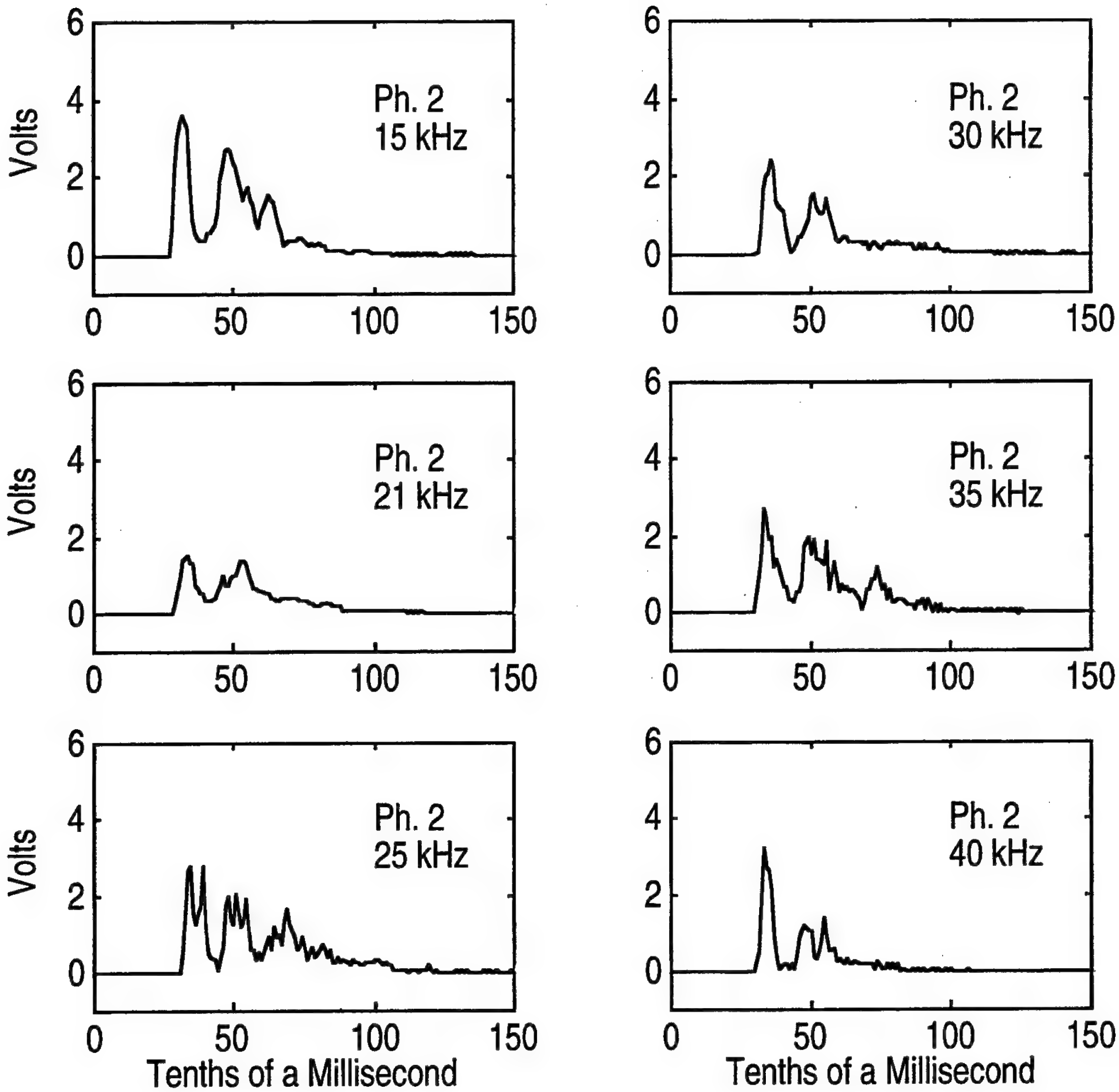

Figure B2. Phone 2 mean envelopes of 0.5 ms pulses.

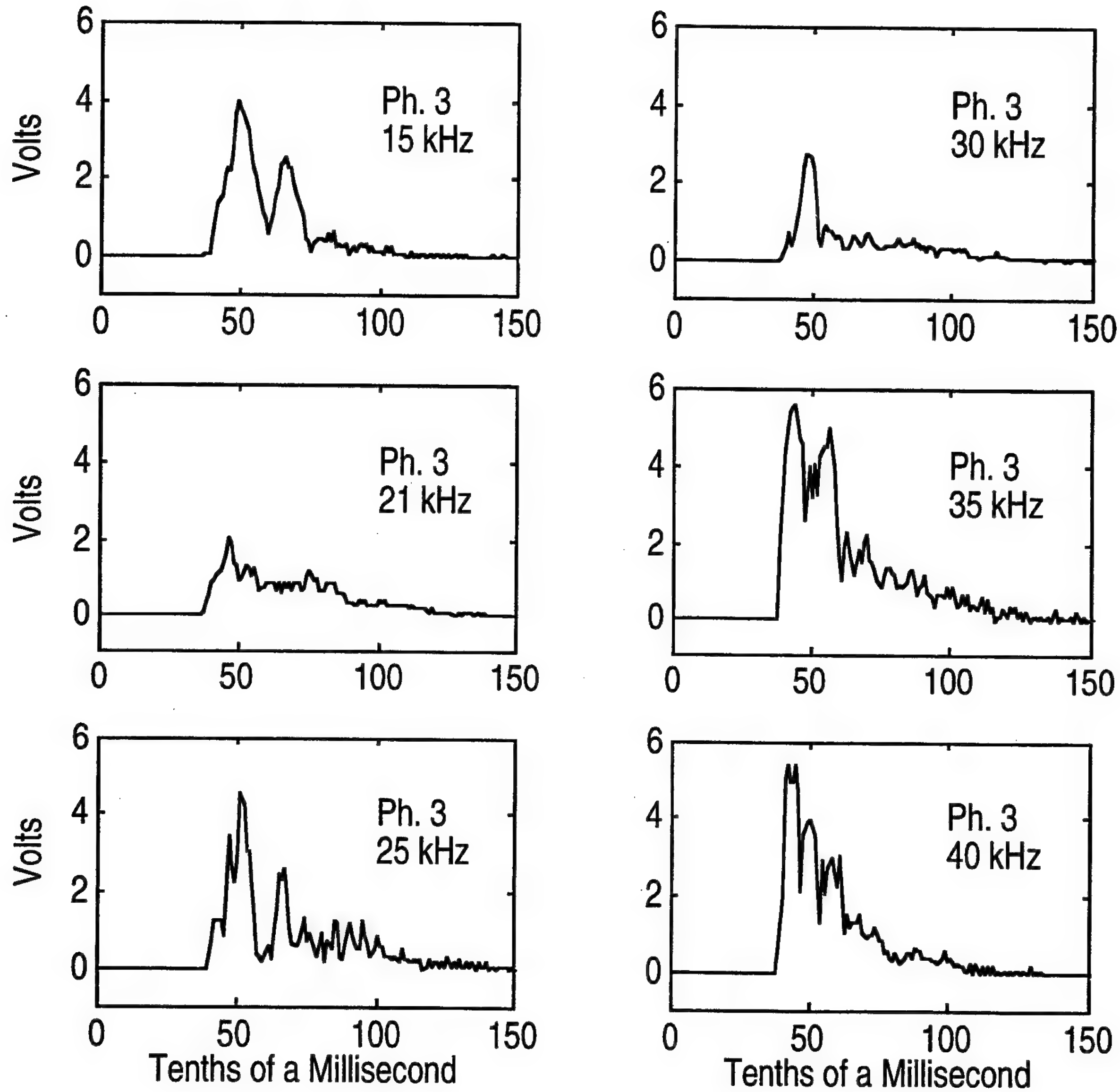

Figure B3. Phone 3 mean envelopes of 0.5 ms pulses.experiment.

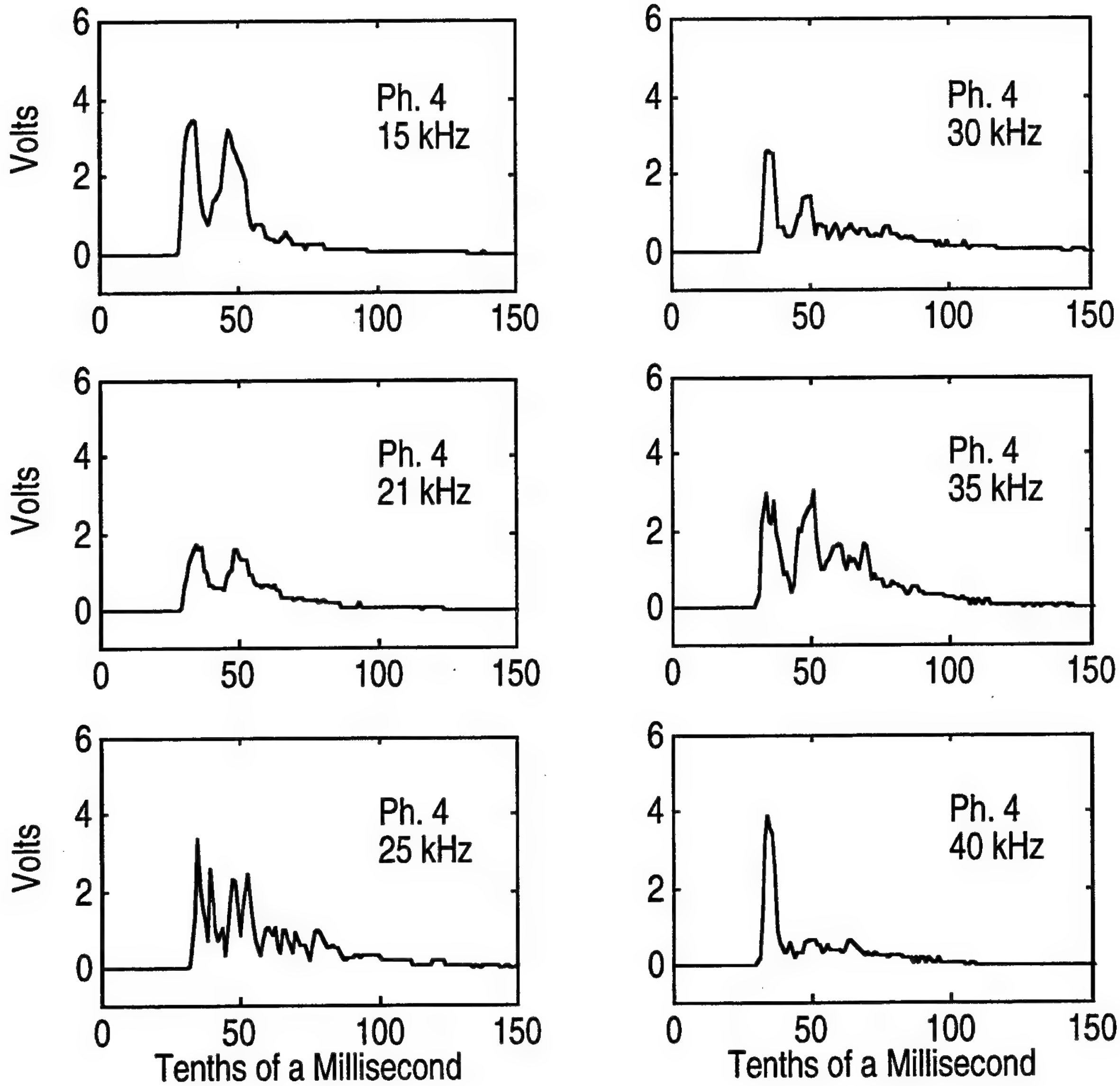

Figure B4. Phone 4 mean envelopes of 0.5 ms pulses.

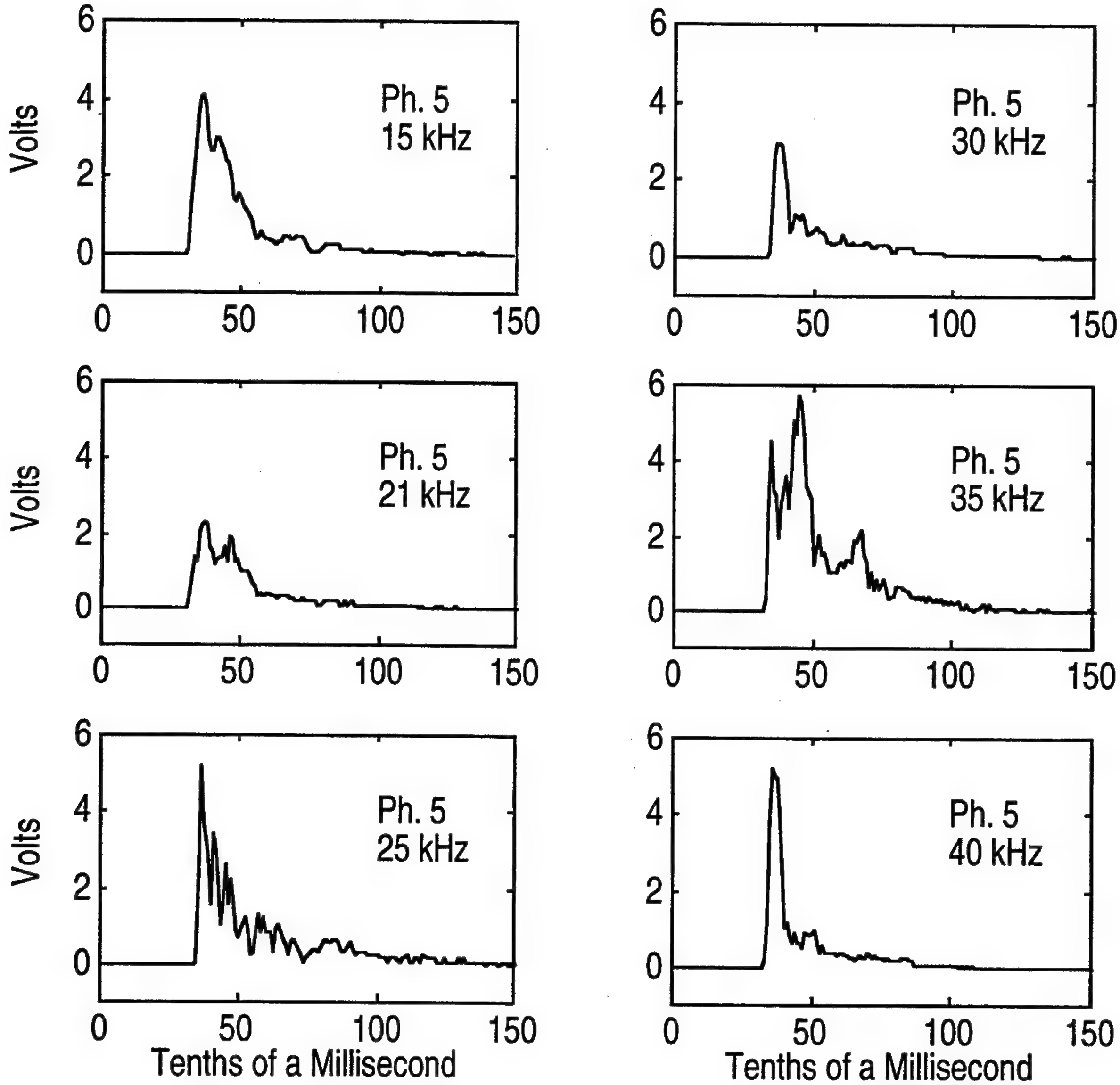

Figure B5. Phone 5 mean envelopes of 0.5 ms pulses.

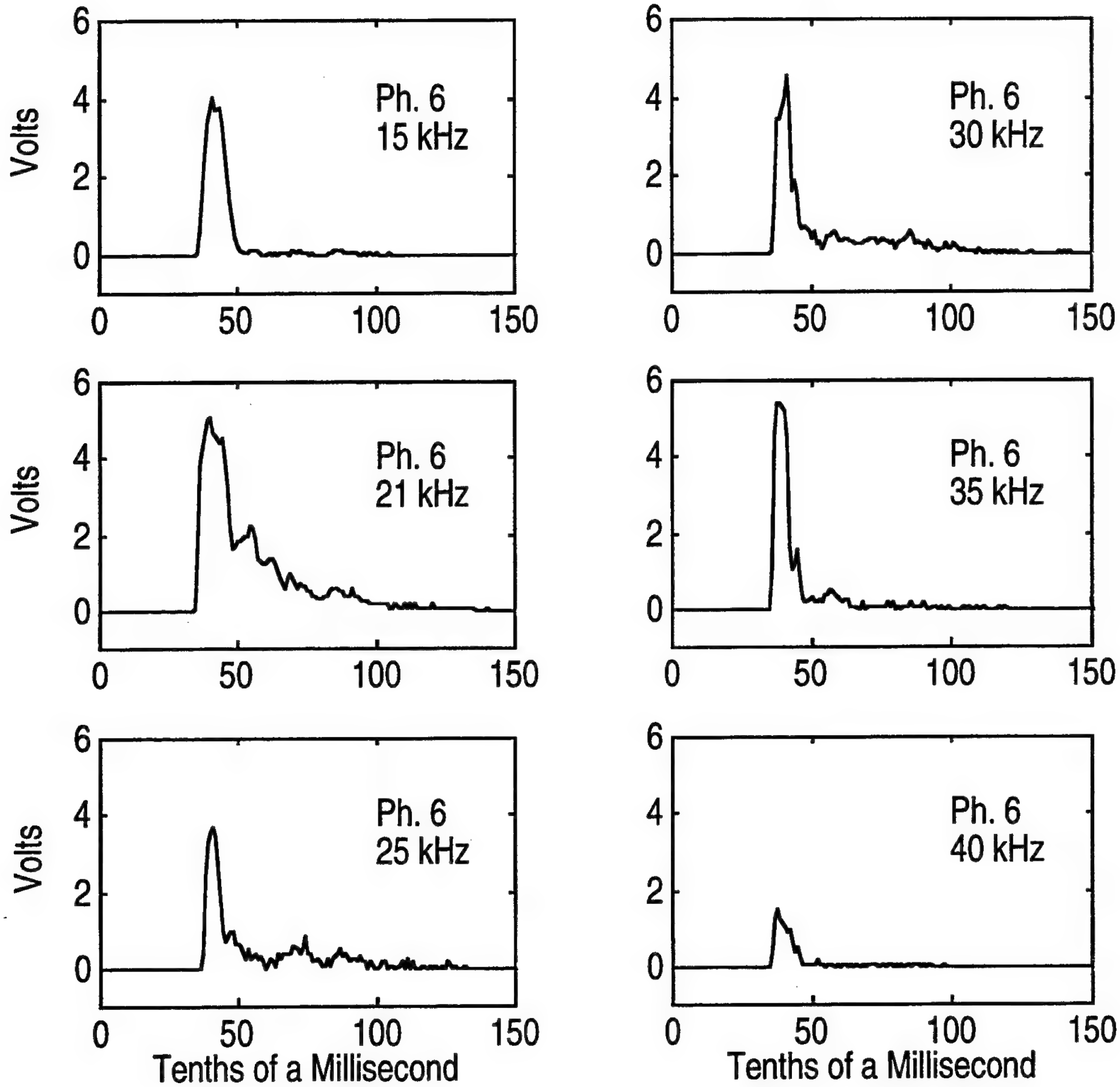

Figure B6. Phone 6 mean envelopes of 0.5 ms pulses.

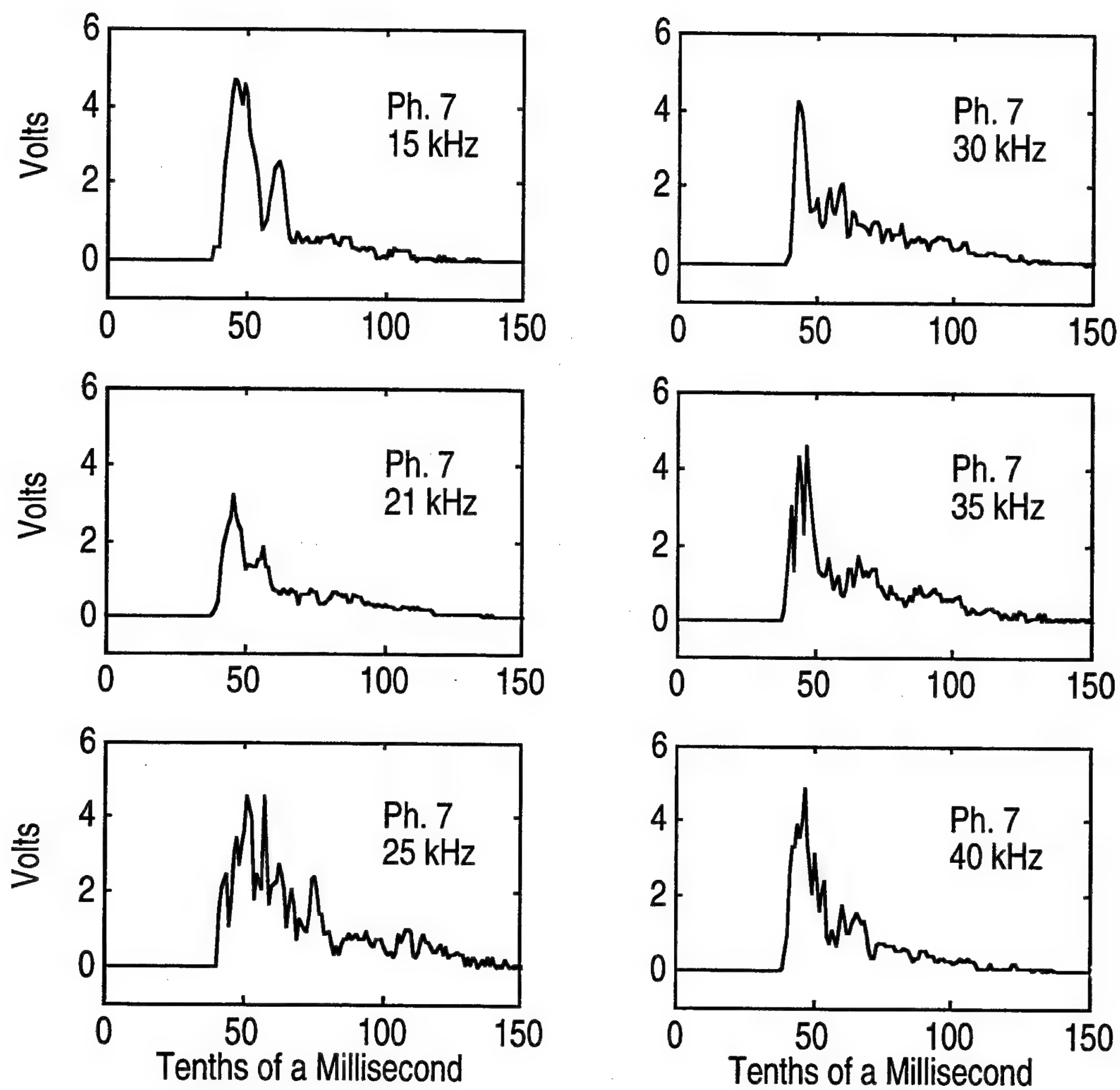

Figure B7. Phone 7 mean envelopes of 0.5 ms pulses.

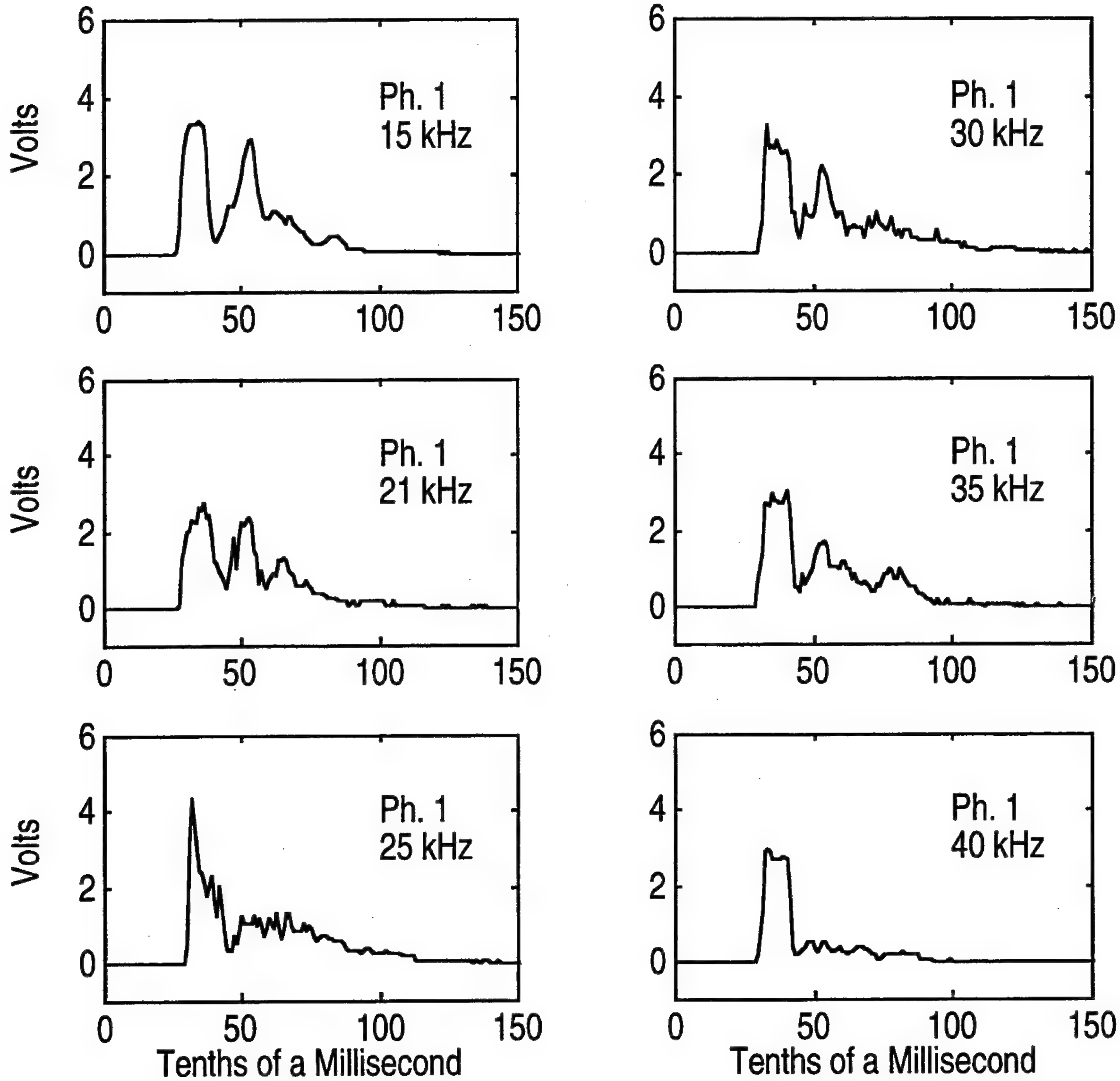

Figure B8. Phone 1 mean envelopes of 1 ms pulses.

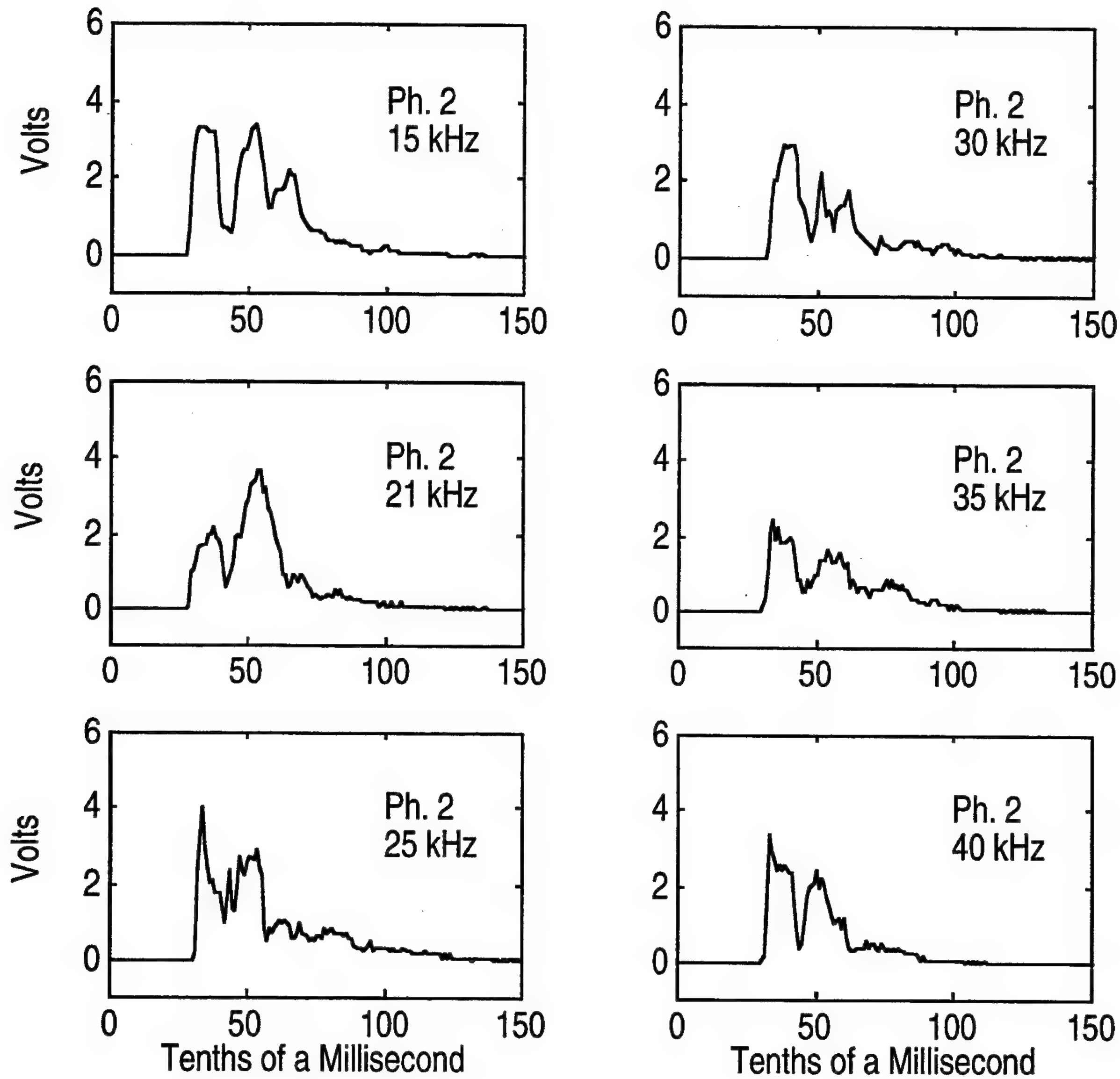

Figure B9. Phone 2 mean envelopes of 1 ms pulses.

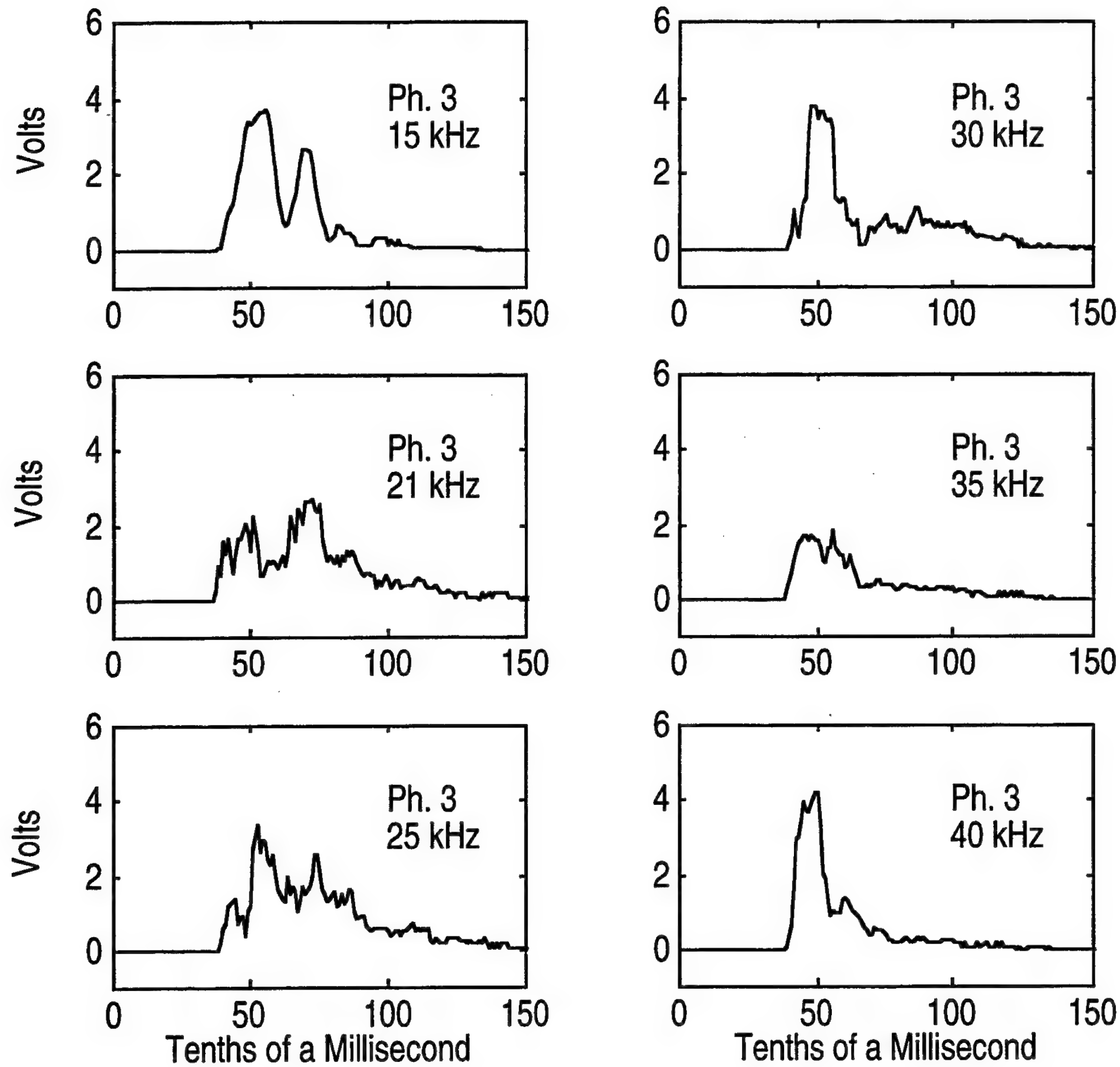

Figure B10. Phone 3 mean envelopes of 1 ms pulses.

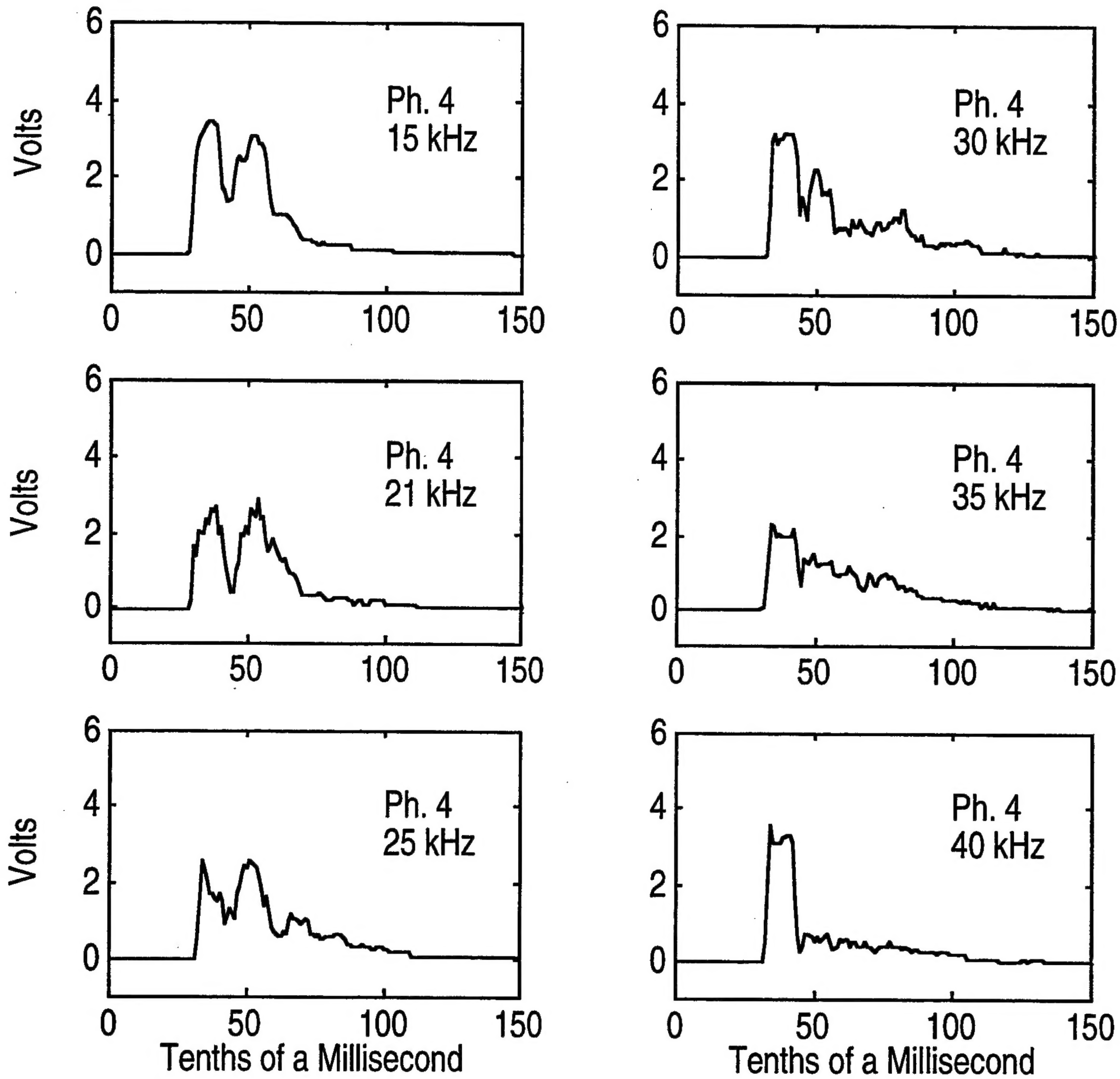

Figure B11. Phone 4 mean envelopes of 1 ms pulses.

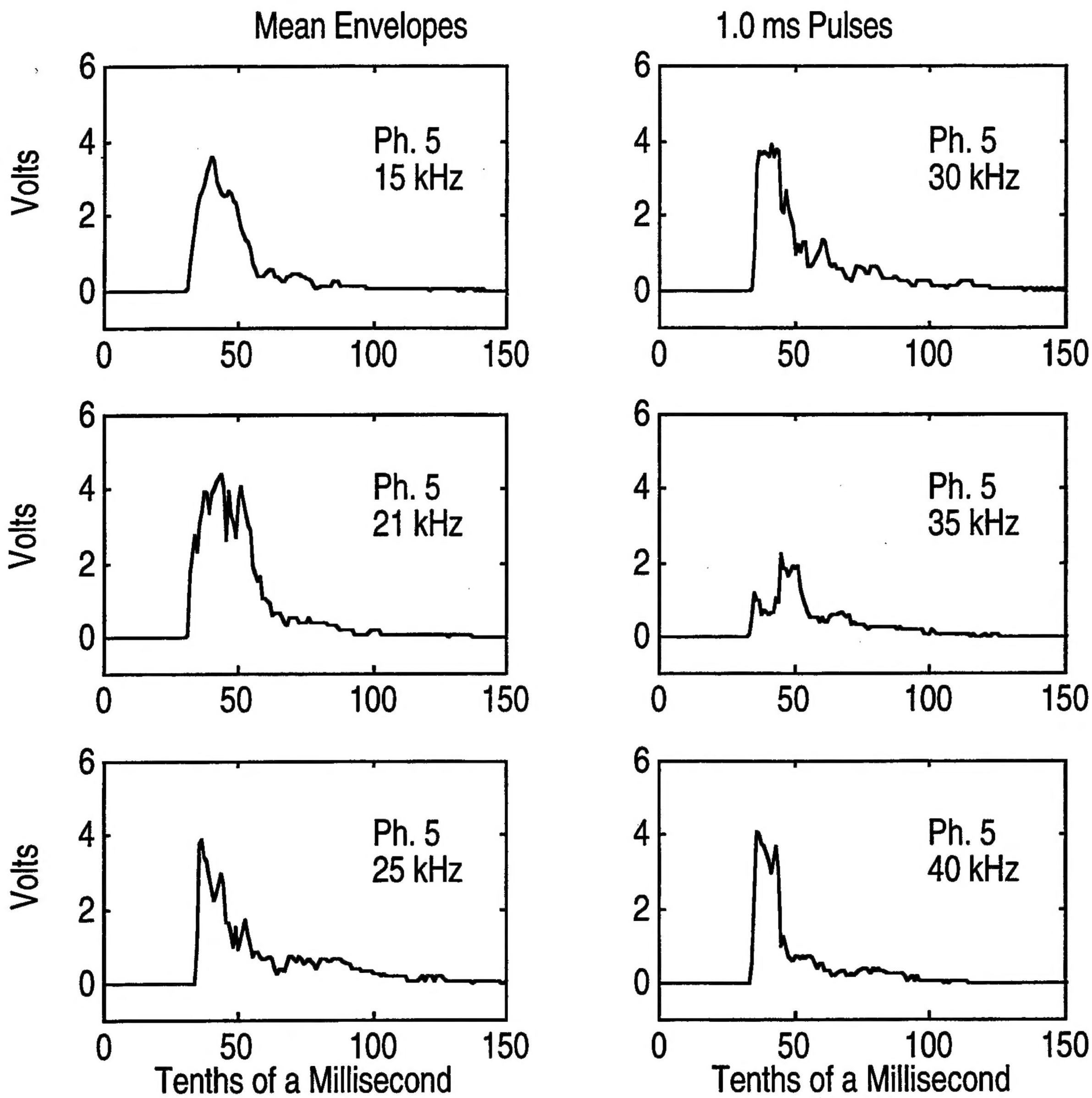

Figure B12. Phone 5 mean envelopes of 1 ms pulses.

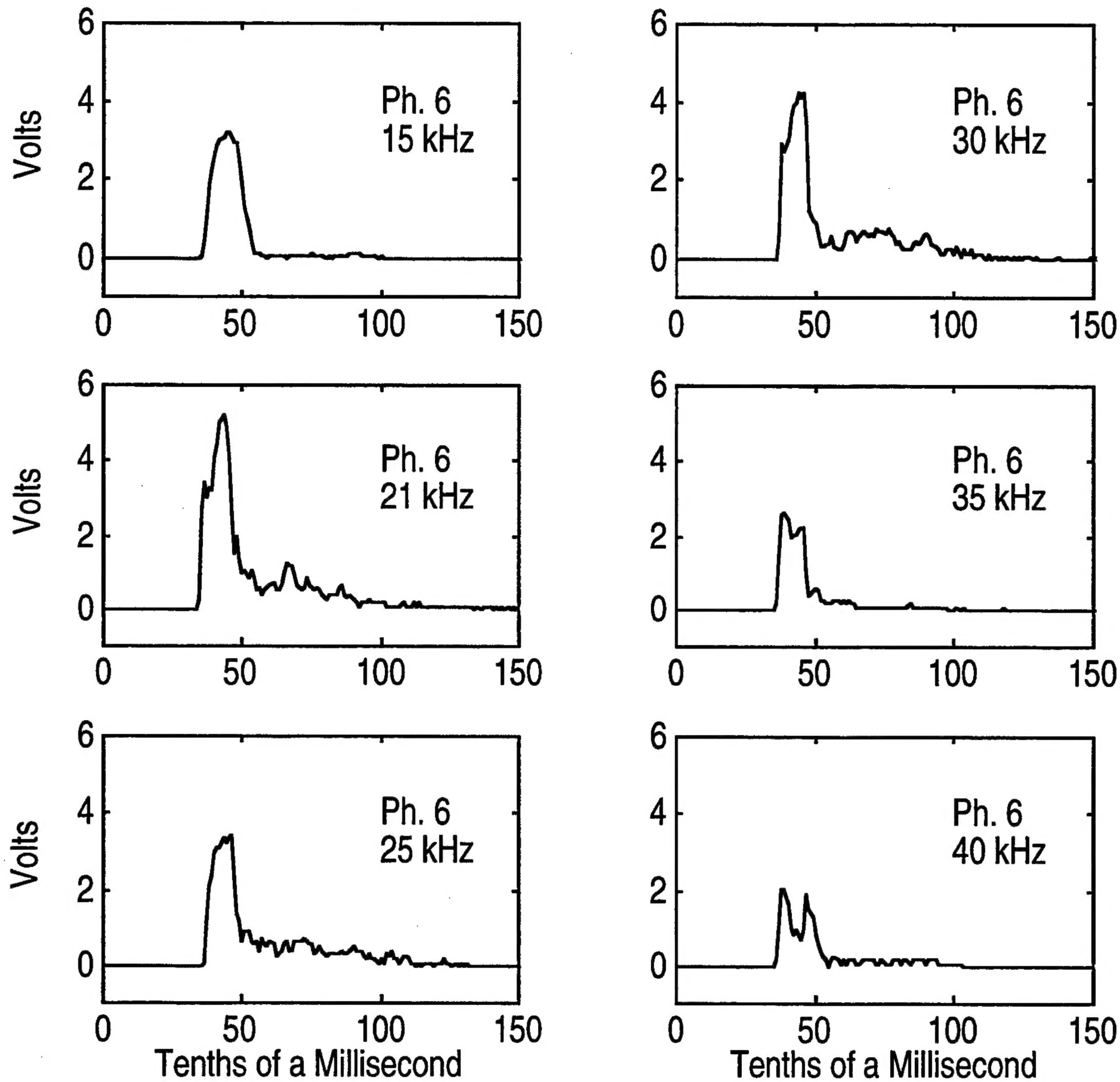

Figure B13. Phone 6 mean envelopes of 1 ms pulses.

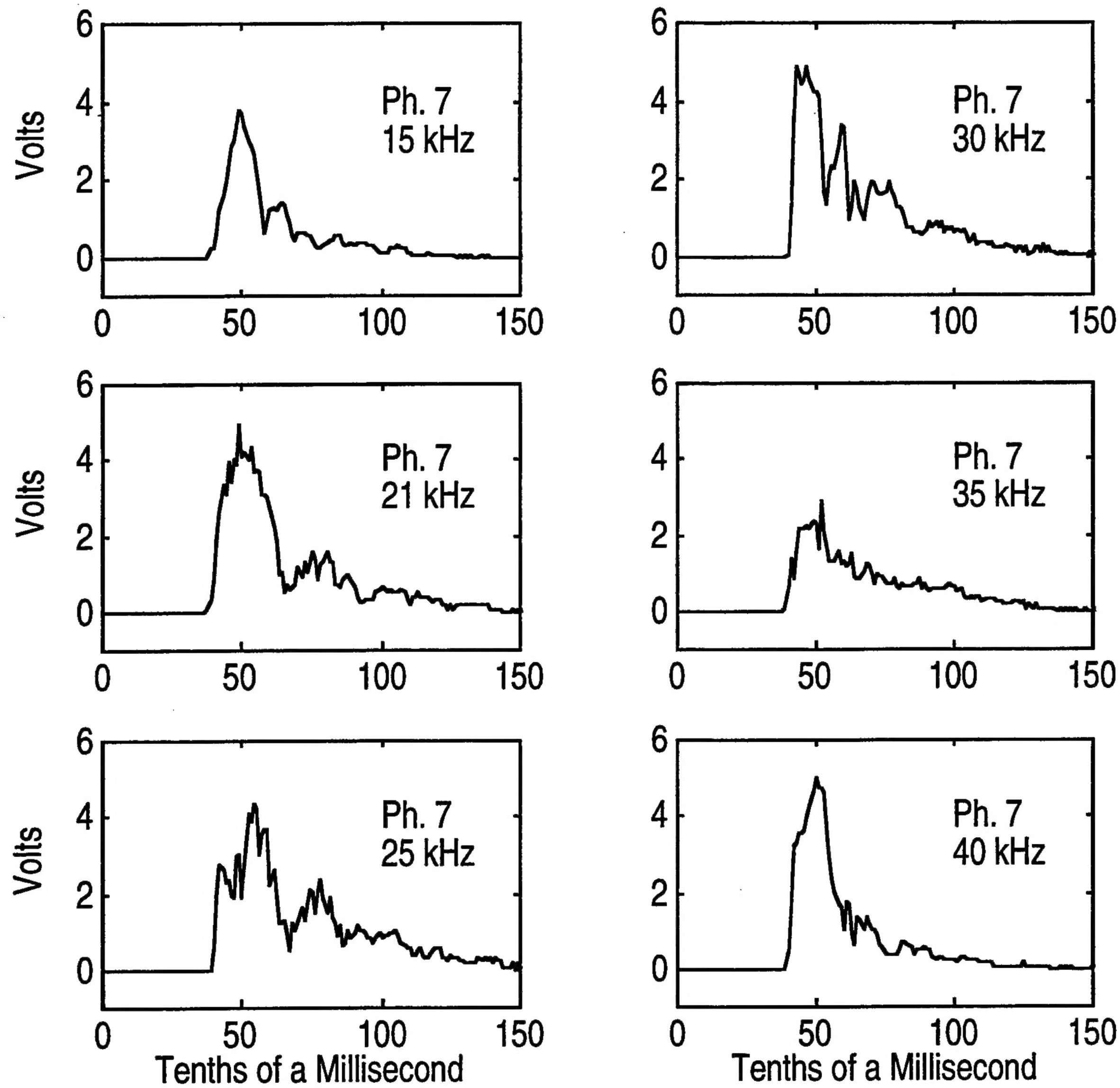

Figure B14. Phone 7 mean envelopes of 1 ms pulses.